Quaternary Geochronology 61 (2021) 101128

Contents lists available at ScienceDirect

Quaternary Geochronology

journal homepage: http://www.elsevier.com/locate/quageo

# Cross-comparison of last glacial radiocarbon and OSL ages using periglacial fan deposits

Sanne W.L. Palstra [a,*], Jakob Wallinga [b], Willem Viveen [c], Jeroen M. Schoorl [b], Meindert van den Berg [d], Johannes van der Plicht [a,e]

[a] Centre for Isotope Research, Energy and Sustainability Research Institute Groningen, University of Groningen, Nijenborgh 6, 9747 AG, Groningen, the Netherlands
[b] Soil Geography and Landscape Group & Netherlands Centre for Luminescence dating, Wageningen University, P.O. Box 47, 6700 AA, Wageningen, the Netherlands
[c] Grupo de Investigación en Geología Sedimentaria, Especialidad de Ingeniería Geológica, Departamento de Ingeniería, Pontificia Universidad Católica de Perú, Av. Universitaria, 1801, San Miguel, Lima, Peru
[d] Retired from TNO/Geological Survey of the Netherlands, the Netherlands
[e] Faculty of Archaeology, Leiden University, Leiden, the Netherlands

ARTICLE INFO

*Keywords:*
Radiocarbon
AMS
OSL
Weichselian
Fan deposits

ABSTRACT

Two cores from a Weichselian periglacial alluvial fan were dated using $^{14}$C and OSL, to verify the reliability of both methods and check the upper dating limit of the $^{14}$C method. Both dating methods yielded a similar chronology for core Eerbeek-I, with infinite $^{14}$C dates for the lower part where OSL dates indicated ages of over 45 ka. Finite $^{14}$C dates were obtained throughout the core for Eerbeek-II, despite stratigraphic and OSL evidence suggesting ages beyond $^{14}$C limits. Apparently, additional chemical pre-treatment to remove younger carbon fractions did not work adequately for samples from this core. We hypothesize that this may be related to a larger influence of younger-age humin fractions in the mainly sandy Eerbeek-II deposits compared to those buffered by a thick peat layer of Eerbeek-I. We suggest that (local) stratigraphy, percolation and humification processes may impact $^{14}$C ages of organic deposits more than commonly assumed, and should receive more attention. In addition, we introduce a new method to assess robustness and validity of OSL dates and demonstrate the applicability of OSL dating methods in this setting. Our results highlight that the $^{14}$C method requires additional verification methods, such as OSL, for deposits older than 30 ka.

## 1. Introduction

Crucial information on the temporal dynamics of terrestrial landscapes is preserved in the sedimentary record. Deposits are stratified, but their structure and composition generally do not give conclusive information about their age and deposition rate. Dating methods such as Radiocarbon ($^{14}$C) and Optically Stimulated Luminescence (OSL) determine the age of specific selected deposits and are therefore essential tools for the interpretation of these geological archives.

The radiocarbon dating method, developed at the end of the 1940s (e.g. Libby, 1952), is based on the radioactive decay of $^{14}$C. The age of a sampled is calculated from the measured $^{14}$C content. The method can be used to date organic materials up to its detection limit of approximately 50 ka, and is also applied to date organic material from deposits (e.g. De Vries, 1958). The OSL dating method was developed in the 1980's (Huntley et al., 1985; Wintle, 2008). The method determines the timing of deposition and burial of sand or silt-sized mineral grains, using the luminescence signal that builds up in quartz or feldspar minerals over time due to exposure to natural background radiation. Luminescence methods are applicable over the age range of a few years (Madsen and Murray, 2009) up to about 150 ka for quartz (Preusser et al., 2008) and up to 500 ka for feldspar (Buylaert et al., 2012).

Combining the results of the $^{14}$C and OSL methods for dating deposits has several advantages. First, different types of deposits and therefore more layers can be dated as a function of depth, as the dating of mineral layers (only by OSL) and layers with organic carbon (only by $^{14}$C) can be combined. And second, consistency and reliability of obtained age-depth profiles can be verified when more than one dating method is used. Robustness of chronologies can greatly profit from the latter, as for both dating methods age anomalies can occur due to several site-specific and methodological factors affecting the suitability and purity of the samples of interest.

* Corresponding author.
*E-mail address:* s.w.l.palstra@rug.nl (S.W.L. Palstra).

https://doi.org/10.1016/j.quageo.2020.101128
Received 19 December 2019; Received in revised form 25 September 2020; Accepted 27 September 2020
Available online 8 October 2020

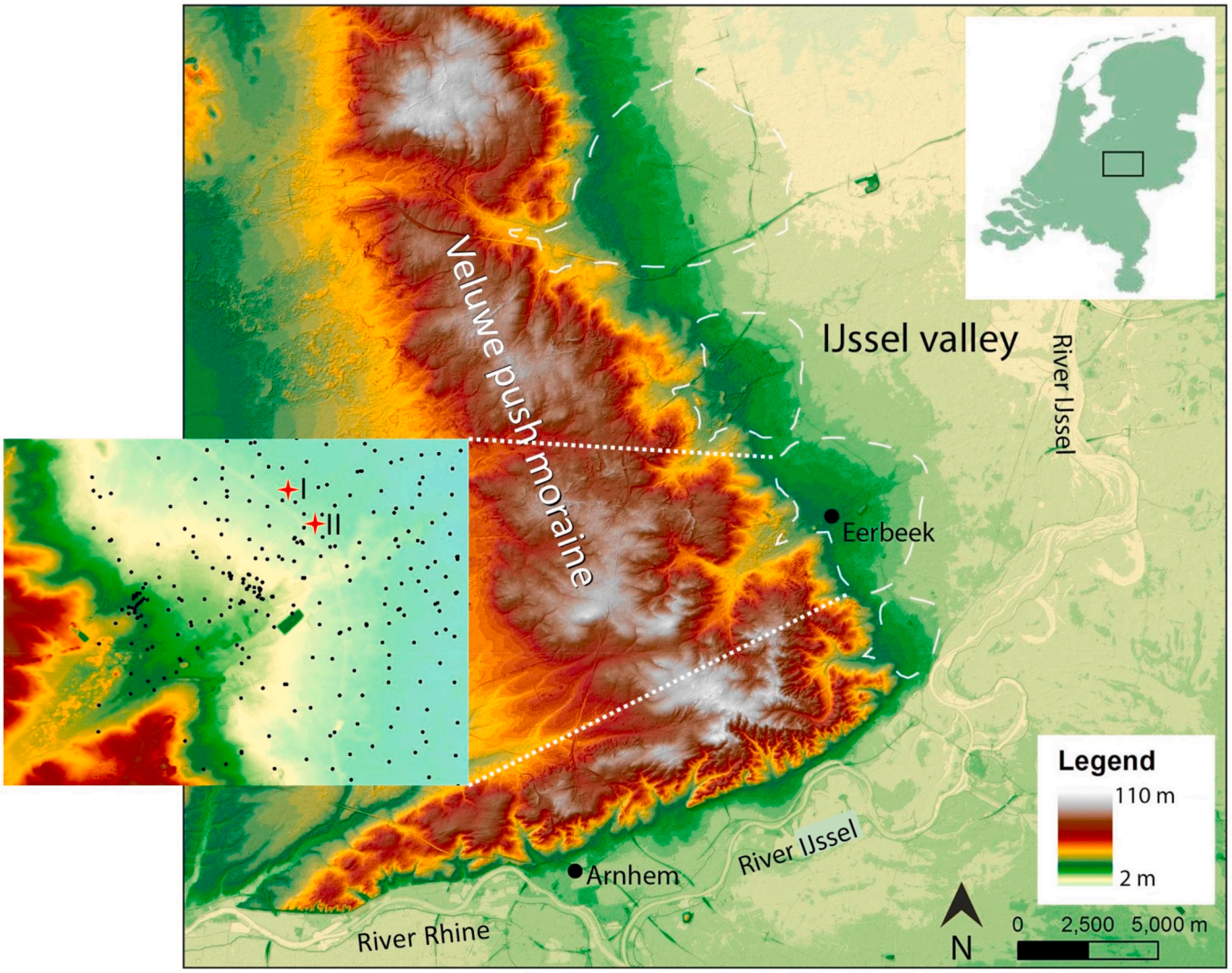


**Fig. 1.** Location of Eerbeek in The Netherlands showing the Veluwe push moraine and outlines of the fans developed on its eastern margin. The inset shows the Eerbeek fan area with, among the dots of other coring sites (DINO, 2014), the locations of the cores discussed in the present study: Eerbeek-I and Eerbeek-II (red stars and 'I' and 'II').

Most combined $^{14}$C-OSL studies so far have dated deposits with ages up to about 25 ka (Vandenberghe et al., 2004; Kolstrup et al., 2007; Demuro et al., 2008; Derese et al., 2009; Crombé et al., 2012; Wallinga et al., 2013; Újvári et al., 2014; Viveen et al., 2019). Only a few studies have combined both methods to date deposits with ages close to or even beyond the detection limit of the $^{14}$C method, 50 ka (Magee et al., 1995; Briant et al., 2005; Briant and Bateman, 2009; Kliem et al., 2013 combined with Buylaert et al., 2013).

In several of these studies $^{14}$C and OSL methods yield contrasting chronologies. The differences observed vary within and between the different studies and do sometimes occur for only a few individual samples, while in other cases inconsistent results are obtained for a whole series of samples. Quite often $^{14}$C dates are younger than OSL dates for the same stratigraphic unit, in particular for deposits older than ca. 30 ka (Magee et al., 1995; Briant et al., 2005; Derese et al., 2009; Briant and Bateman, 2009; Kliem et al., 2013). In contrast, for younger deposits formed during the Late Glacial or Holocene, $^{14}$C ages older than those obtained by OSL are observed as well (Kolstrup et al., 2007; Crombé et al., 2012; Wallinga et al., 2013).

A main difficulty in $^{14}$C dating of organic deposits is the mixing of this material with carbon from other origins and ages. It can be very hard to remove these added carbon fractions. Chemical pre-treatment of organic deposit material is a challenging feature here (Briant and Bateman, 2009; Wallinga et al., 2013; Briant et al., 2018).

OSL dating requires accurate determination of both the burial dose and dose rate. Age underestimation may arise when dose rates are overestimated and/or burial doses are underestimated. The former may for instance occur if water contents are underestimated (Kolstrup et al., 2007), while the latter may occur towards saturation of quartz OSL (Anechitei-Deacu et al., 2018). Overestimation of the burial age may occur if dose rates are underestimated, but are more likely caused by overestimation of burial dose related to limited light exposure prior to deposition and burial, resulting in incomplete resetting of the OSL signal. However, in many cases this problem can be mitigated or circumvented through the use of appropriate statistical treatment to derive a burial dose from the equivalent dose distribution (e.g. Galbraith et al., 1999; Cunningham and Wallinga, 2012).

The main aims of this study are to demonstrate the advantages and challenges of combining $^{14}$C and OSL methods and to check the accuracy of the pre-treatment for $^{14}$C dating close to its detection limit for terrestrial plant macrofossils. In other published studies in which $^{14}$C and OSL were combined and compared for ages >25 ka, either only one stratigraphic record was investigated (Magee et al., 1995; Kliem et al., 2013 combined with Buylaert et al., 2013), or different sites were

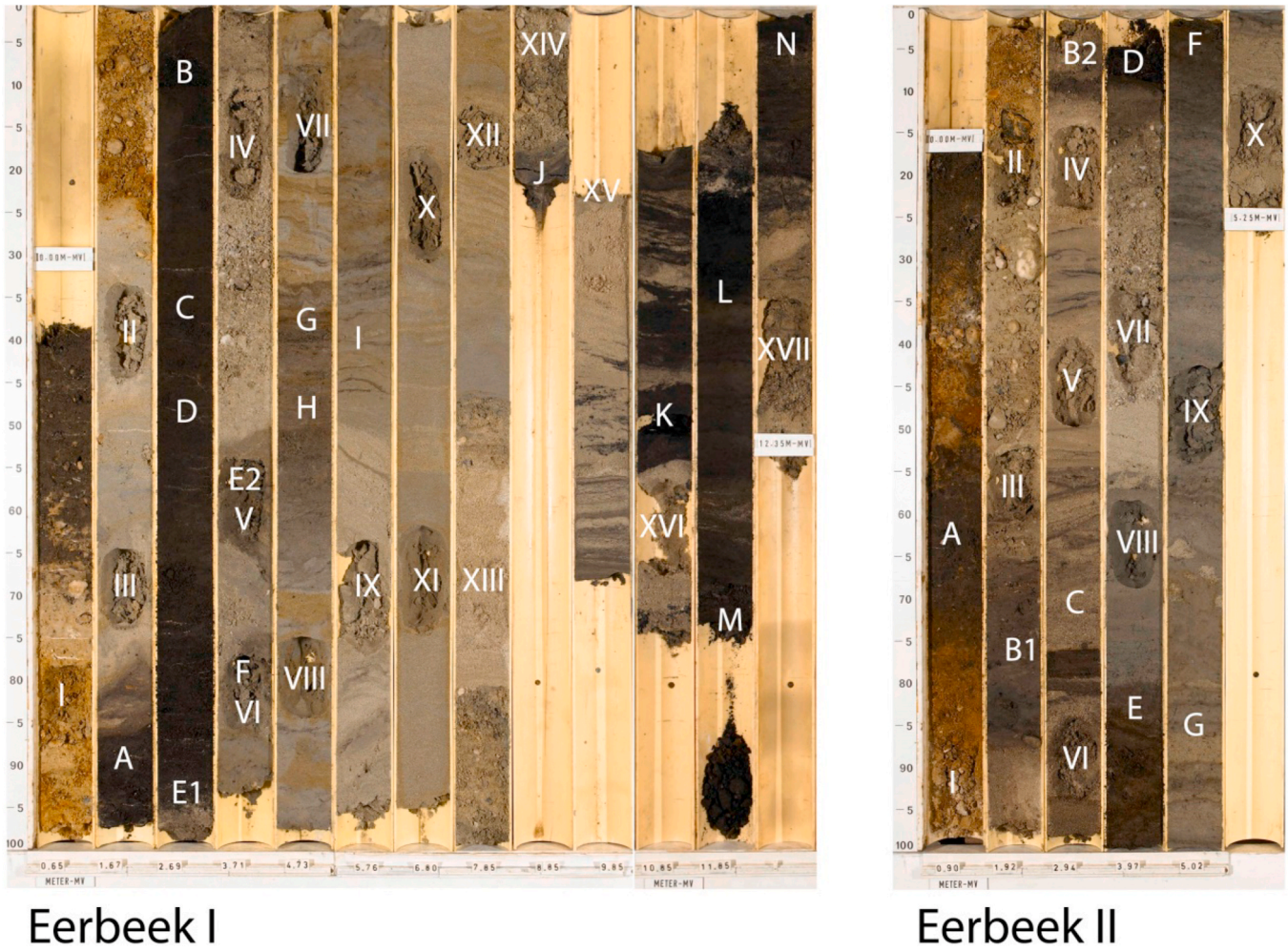


**Fig. 2.** Sampled cores of Eerbeek-I and Eerbeek-II. The OSL samples have Roman numbers; the $^{14}C$ samples are indicated with capital letters.

investigated but then only at limited specific stratigraphic sections (Briant and Bateman, 2009). The current study demonstrates a completely sampled stratigraphic record of two cores obtained from two geographically different sites, which have a similar regionally determined stratigraphy. The results therefore demonstrate for both $^{14}C$ and OSL dating methods whether age-depth profiles can be reproduced for cores with similar stratigraphy.

## 2. Site and methods

For this study, two drilled cores with both clastic and organic deposits were dated. The cores were obtained from a Weichselian alluvial fan near Eerbeek, The Netherlands. Based on previous studies of this fan (Kolstrup and Wijmstra, 1977; van der Meer et al., 1984), part of the investigated sequence was expected to be older than 50 ka, which allowed establishing the age limit of the $^{14}C$ method for this kind of deposits.

### 2.1. Geological setting

In The Netherlands ice-pushed ridges are prominent topographic features up to 100 m above sea level. These ridges were shaped by inland ice-sheets during the Late MIS 6 stage (ca. 140.000 years ago) and they consist primarily of displaced fluvial sandy deposits (Van den Berg and Beets, 1987; Bakker and Van der Meer, 2003; Busschers et al., 2008). A brief summary is given here of the erosion history of the ridges and associated formation of fan-shaped deposits covering the foot-slopes of the ridges, based on studies by Maarleveld (1949) and van der Meer et al. (1984). As the sandy deposits are highly permeable, surface runoff was limited unless permafrost conditions hampered infiltration. Consequently, surface erosion in the push moraine-fan catchment area was probably negligible during the Eemian (MIS 5e). Precipitation infiltration in combination with an elevated ground water table due to a higher sea level, created marshy conditions in the seepage zone at the outer part of the fan (De Mulder et al., 2003). This resulted in the development of deposits with high organic matter content in those areas, while other parts of the fans showed little morphological change (van der Meer et al., 1984). Surface erosion in the fan catchment areas and sedimentation on the fan surfaces was initiated during the following Weichselian (MIS 5d – MIS 2) glacial with permafrost conditions, until the onset of the Holocene. During the Weichselian, climate conditions frequently changed from dry to wet and cold to warm (Kasse et al., 1995; Aalbersberg and Litt, 1998; Bateman and van Huissteden, 1999). This resulted in episodic alluvial fan activity, the formation of aeolian cover sands (Kasse, 2002) and avulsions of the nearby River Rhine (Busschers et al., 2008). As a consequence, subsurface conditions frequently changed in the alluvial fan areas during the Weichselian, resulting in a stratigraphic sequence of coarse and fine-grained alluvial fan deposits, aeolian sands, and alluvial-lacustrine peat, loam and clay deposits (Kolstrup and Wijmstra, 1977; Ruegg, 1979; van der Meer et al., 1984; Den Otter, 1989). Cores taken from these fans therefore contain both clastic and organic deposits.

### 2.2. Site selection and sampling

The two cores dated in this study were drilled near the Late Pleistocene IJssel valley, from a fan near the Dutch village of Eerbeek (Fig. 1). This fan was selected because the stratigraphy was already known in general terms from previous studies (Ruegg, 1979; van der Meer et al., 1984; Den Otter, 1989) and more recently, a reconstruction of the stratigraphy of the entire Eerbeek fan on the basis of electric cone-penetration tests (CPTs) was made (Viveen, 2005). This method uses information on the sleeve friction and the cone resistance to investigate sediment properties, for instance organic matter and grain size (Douglas and Olsen, 1981; Lunne et al., 1997). Because for the comparison of the OSL and $^{14}C$ dating methods a stacked sequence of intercalated organic and inorganic layers was required, two sites were selected on the basis of those CPT results (Viveen, 2005, CPT data available through DINO, 2014).

The two selected core sites 'S33G0060' (location code: '32U 29971 5778076') and 'S33G0063' ('32U 300185 5777499') were located 650 m apart (Fig. 1), and are expected to have a similar stratigraphy based on CPT transects. A detailed description and a (visual) comparison of the lithology and sedimentary structures of the two dated cores are given in the Results section.

In this paper the two cores are referred to as 'Eerbeek-I' and 'Eerbeek-II' respectively. The cores were drilled in 2009 by GeoDelft/Deltares using a mechanical bailer-drilling unit with the possibility of retrieving undisturbed continuous cores supported by a PVC-liner (following the 'Begemann augering' technique, Begemann, 1974). The cores were subsequently cut into 1-m long sections and stored in PVC-tubes. When deeper continuous coring was no longer possible, the core was extended using a piston corer that retrieves samples in sections of approximately 1-m length.

Coring proved to be cumbersome due to the presence of gravel. At Eerbeek-I, the Begemann auger tip broke off at 8 m depth and the core could only be extended down to 12.4 m below the surface using the piston corer. The borehole had to be cleaned after each attempt, resulting in recovery loss. At 12.4 m depth, the piston corer tip broke off as well, effectively ending any further drilling. At Eerbeek-II, the Begemann auger tip struck a gravel bed at 5.3 m depth, and broke off. Subsequent attempts with the piston corer to go deeper were unsuccessful.

The cores were sealed and transported to the laboratory of the Netherlands Centre for Luminescence dating (NCL), at that time located at Delft University of Technology. Under safelight conditions of the NCL laboratory, the cores were opened and split in two. One half was used under daylight conditions for descriptions of sedimentology and stratigraphy (Fig. 2). The other half remained in the dark room laboratory where clastic intervals were sampled for OSL dating by NCL. The more organic intervals were also sampled from this half and brought to the University of Groningen (Centre for Isotope Research) for $^{14}C$ dating.

### 2.3. $^{14}C$ dating method

The Centre for Isotope Research, University of Groningen dated thirteen Eerbeek-I and eight Eerbeek-II deposit samples by $^{14}C$. Specific organic fractions were selected from the deposits and chemically pre-treated. The pre-treated material was then combusted to pure $CO_2$ and transferred into graphite. An Accelerator Mass Spectrometer (AMS) measured the isotope ratios $^{14}C/^{12}C$ and $^{13}C/^{12}C$ of the graphite. From these measurements the age of the organic deposits was calculated. Details are given below.

#### 2.3.1. Selection and chemical preparation of organic material

Plant remains (small pieces of plant branches, leaves and seeds) were selected from each sample to ascertain that the dating material originated from the specific deposit during its formation. No attempt was made to identify plant species present, although for some sub-samples specific plant remains were selected (see section 2.3.2). Roots that could be identified in upper deposits (<1 m depth) were removed to decrease possible contamination with carbon from more recent plants. Each soil sample was washed with tap water and sieved over a 600 μm sieve to select only the larger fragments of plant remains. The main aim of this separation step based on particle size was to remove (smaller) organic particles that could have been transported into the deposit from deposits with another age. Sand and clay particles were also washed out during this sieving process. Remaining gravel, if present, was removed by hand. The plant remains were dried in a stove at 100 °C and stored in small glass flasks until further sample preparation.

**Table 1**
Applied chemical pre-treatment in this study.

| Method | Step 1 | Step 2 | Step 3 | Applied to samples |
|---|---|---|---|---|
| Light ABA | 1 M HCl, 100 °C, 24 h | 1.1 M NaOH, 20 °C, 5 min | 1 M HCl, 100 °C, 24 h | EB-I: A, B, C, D E1, E2, G, H, K, M; EB-II: A, B1, C, D, E, F, G |
| Light ABA + Mild BA ('+') | Light ABA | 0.25 M NaOH, 50 °C, 2 h | 1 M HCl, 20 °C, 168 h | EB-I: A+, C+, D+, H+; EB-II: B1+, C+, D+, E+, F+, G+ |
| Light ABA + Mild BA + Strong BA ('++') | Light ABA + Mild BA | 1.5 M NaOH, 90 °C, 6 h | 1 M HCl, 20 °C, 4 h | EB-II: F++ |

After the physical selection of plant remains from each sample, a chemical pre-treatment was applied to remove contaminating (younger or older) carbon-containing molecules. Especially humic and fulvic acids are relatively easily (pH dependent) transported by percolating water and may end up in layers other than where they originated from. These foreign carbon molecules alter the overall $^{14}C$ age of the investigated deposits if not removed properly before the actual $^{14}C$ measurement. For the removal of these kinds of carbon contamination the chemical 'ABA pre-treatment' was applied (Mook and Streurman, 1983). In this pre-treatment method selected plant remains are sequentially washed in Acidic, Base and Acidic solutions (ABA).

The concentration of the acid and base (alkaline) solutions, the applied temperatures and the duration of the reaction with the investigated materials all affect the efficiency to remove specific carbon contaminations. These chosen conditions usually vary per sample depending on the type and size of the sample material. Especially in the base step, solid organic materials dissolve well at higher temperature and at increased base concentrations. For part of the investigated Eerbeek samples, the base step was adjusted to lower (room) temperatures and shorter duration to prevent dissolving of the entire carbon sample. Table 1 summarizes the chemical pre-treatment methods that were applied to the samples in this study. Subsamples of ABA-pre-treated sample material were subjected to additional 'mild' (indicated with '+') and 'strong' ('++') alkaline treatments to investigate the effect of a more thorough base step on the measured ages. After each HCl or NaOH treatment the sample material was rinsed thoroughly with decarbonized water. The duration of step 3 of the 'Light ABA + Mild BA' method was one week (168 h). This period was selected purely for logistic reasons; there is no methodological necessity for such a long duration. After the chemical pre-treatment the sample material was dried in a stove at 100 °C and stored in small glass flasks.

#### 2.3.2. Carbon preparation and $^{14}C$ analysis

After chemical pre-treatment, 4–5 mg subsample was weighed in a small tin capsule. For each deposit sample the subsample was a random mixture of different small pieces of the selected and pre-treated plant remains (see Appendix A Table A.1 Table A.2). In a few cases additional subsamples of specific plant remains were measured to investigate

carbon age inhomogeneity between different plant materials of the same deposit. For sample 'Eerbeek I–C' a piece of wood material (10 mm) was pre-treated together with the other plant remains, and then measured separately. For sample 'Eerbeek I–H', a subsample of seeds of one particular species was selected for separate $^{14}C$ measurement.

Each subsample was combusted to $CO_2$ in an Elemental Analyser (EA). Part of this $CO_2$ was led to an IRMS (Isotope Ratio Mass Spectrometer) to measure $\delta^{13}C$. The remaining $CO_2$ was cryogenically trapped and graphitized. The graphite was pressed in targets (Aerts-Bijma et al., 2001) and measured with an AMS. The Groningen AMS instrument used for the samples of this project was a $^{14}C$-dedicated 2.5 MV Tandetron, manufactured by High Voltage Engineering Europe (van der Plicht et al., 2000). The laboratory code for this AMS facility is GrA. This instrument was replaced in 2017.

The $^{14}C$ samples in this study were measured in different AMS-batches. Each AMS batch, consisting of 59 targets, included also a set of calibration and reference materials. The average value of the measured $^{14}C/^{12}C$ ratios of the Oxalic Acid II (SRM-4990C) was used to calibrate the measured $^{14}C/^{12}C$ ratio of an unknown sample to a specific relative $^{14}C$ amount. This $^{14}C$ amount was calculated relative to a defined and standardized $^{14}C$ level for the year 1950 CE. The accuracy of the calibration with Oxalic Acid II was checked in each AMS batch based on the measurement of one or two reference materials with known $^{14}C$ amount. The measurement of an AMS batch was approved if the obtained value of this reference sample was in agreement with its assigned value (within 3-sigma long-term measurement uncertainty).

Each AMS batch also contained a set of three to four $^{14}C$-free pre-treated (ABA) anthracite targets, to determine and correct for the background $^{14}C$ measurement level. The measured average background signal (average $^{14}C/^{12}C$ ratio) of an AMS-batch was subtracted from the measured $^{14}C$ signal ($^{14}C/^{12}C$) of each sample in the calculation of the $^{14}C$ amount (the $F^{14}C$ value, see below). The calculated $^{14}C$ amount was also corrected for isotope fractionation by normalizing the measured $\delta^{13}C$ value to −25‰.

The standardized, normalized and background corrected relative $^{14}C$ amount in each sample, is symbolized with $F^{14}C$: the fraction of $^{14}C$ relative to the standardized $^{14}C$ amount for the year 1950 CE (which has $F^{14}C = 1.0$ by definition). From this number the $^{14}C$ age was calculated using, by convention, the 'Libby half-life' for $^{14}C$ of 5568 years:

$$^{14}C \ \ age = -(5568/1n2)*1n\left(F^{14}C\right) \quad (1)$$

The conventional $^{14}C$ age is expressed in the unit 'BP' ('Before Present') and needs to be calibrated to obtain absolute ages. To calibrate this radiocarbon age to calendar age, the program OxCal (Bronk Ramsey, 2009; used version: 4.3) and calibration curve 'IntCal13' (Reimer et al., 2013) were used. The obtained calendar ages in this study are reported in 'calBP', i.e. the number of calendar years before 1950 CE.

For more details on the calculation of $^{14}C$ and all definitions, conventions and standardizations, see Stuiver and Polach (1977), Mook and van der Plicht (1999), and van der Plicht and Hogg (2006).

**Table 2**
SAR procedure for equivalent dose determination.

| | Action | Measured |
|---|---|---|
| 1 | Beta dose (or Natural dose) | |
| 2 | 10s preheat to 240 °C | |
| 3 | 20s blue stimulation at 125 °C | $L_n$, $L_i$ |
| 4 | Beta test dose | |
| 5 | Cutheat to 220 °C | |
| 6 | 20s blue stimulation at 125 °C | $T_n$, $T_i$ |
| 7 | 40s blue bleach at 250 °C | |
| 8 | Repeat step 1–7 for a range of doses (incl. zero and repeat dose) | |
| Extra 1 | Repeat step 1–7 with added infrared bleach at 30 °C prior to step 3 | |
| Extra 2 | Linearly Modulated OSL following 25 Gy dose and preheat | |

### 2.4. OSL dating

Optically Stimulated Luminescence (OSL) dating determines the last exposure of natural mineral grains to daylight, and thereby the time of deposition and burial of sediments. For this dating method two quantities need to be determined.

Firstly, the burial dose. This is the total amount of ionizing radiation received by the sample since the last exposure to light. The estimation of this burial dose is also referred to as 'palaeodose', which is obtained through statistical interpretation of the equivalent dose distribution. Equivalent doses are determined using luminescence measurements on small subsamples of prepared mineral fractions of the investigated sample.

Secondly, the (average) amount of ionizing radiation absorbed per year must be estimated for each sample. This absorption rate is referred to as 'dose rate' and is calculated from the measured radionuclide concentrations of the sample and its surrounding, taking into account attenuation effects of moisture and organic material, and adding a small contribution from cosmic rays. Details are given below.

#### 2.4.1. Selection of sediment samples

Sediment samples of about 500 g were taken from the core under subdued orange/amber light conditions in the laboratory of the Netherlands Centre for Luminescence dating (NCL). This sample size provided sufficient material for both the equivalent-dose and the dose-rate measurements. To allow straightforward calculation of the dose rate using the infinite matrix assumption (Aitken, 1985), samples were preferentially taken from intervals without clear lithological boundaries within 20 cm from the sample. Sections with clear sedimentary structures were preferred as their presence provided evidence that the material was not disturbed during sampling. Seventeen samples were taken from core Eerbeek-I, and another ten samples from Eerbeek-II. A subset of twenty-one samples was selected for OSL dating: twelve from Eerbeek-I and nine from Eerbeek-II. These samples were split in two parts in the NCL laboratory: one part was prepared for dose-rate analysis and the other part for equivalent-dose measurements (estimation of the burial dose).

#### 2.4.2. Pre-treatment of sediment samples for burial dose estimation

In this study the burial dose estimation is based on luminescence measurements of quartz grains. To obtain purified quartz separates the selected samples were prepared by sieving and chemical treatment. First, the 180–212 μm sand fraction was obtained by wet sieving. This fraction was then treated with HCl (10%) and $H_2O_2$ (30%) to remove carbonates and organic materials. The cleaned sample was then treated with concentrated HF (40%) to dissolve feldspar grains and etch away the alpha-exposed outer rim of the quartz grains. The quartz separates were washed with diluted HCl and water, and then sieved again to remove those grains that were severely affected by the HF treatment. By monitoring the response to infrared stimulation the purity of the quartz separates was checked (Duller, 2003). If needed, the HF etching step was repeated.

#### 2.4.3. Burial dose estimation

For burial dose estimation, a set of small subsamples (aliquots) of purified quartz grains were prepared for each sample. The aliquots were prepared with a monolayer of grains on a stainless-steel disc sprayed with a thin layer of silicon spray. The prepared grains were mounted only on the centre 2 mm of the sample discs in order to detect incomplete resetting (e.g. Wallinga et al., 2002) and to avoid increased scatter due to heterogeneous beta sources during luminescence measurements (Ballarini et al., 2006).

Luminescence measurements were performed with Risø TL/OSL-DA-15/20 readers equipped with internal $^{90}Sr/^{90}Y$ beta sources and blue (470 nm) and infrared (860 nm) LEDs (Botter-Jensen et al., 2003). Quartz OSL signals are composed of a number of components, which

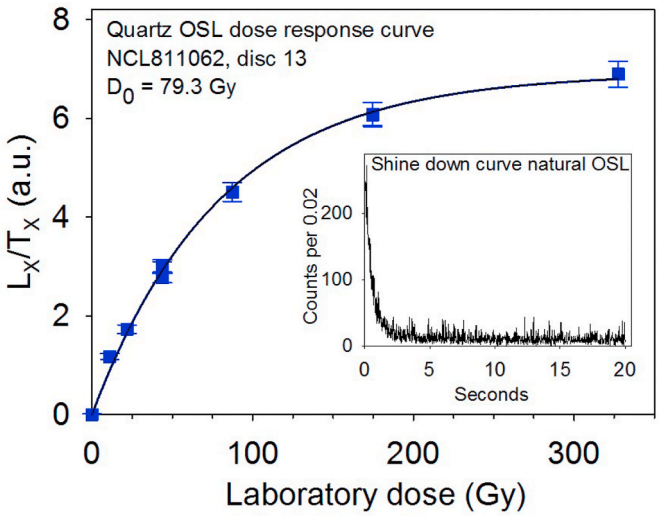


**Fig. 3.** Examples of an OSL dose response curve (main figure) and OSL decay curse (inset: 'shine down curve').

decay at different rates when exposed to light (Bailey and Arnold, 2006). The light-sensitive fast-OSL component is most suitable for dating (e.g. Wintle and Adamiec, 2017), and to optimize the contribution of this component in the signal used for analysis, we applied an early background subtraction (Cunningham and Wallinga, 2010), with a net signal obtained from the signal in the first 0.5 s of stimulation, minus the normalized 'background' between 0.5 and 1.75 s. This net signal is referred to as 'OSL signal' from here on.

The Single-Aliquot Regenerative (SAR) dose procedure (Murray and Wintle, 2000, 2003) was applied for equivalent-dose measurement. Suitable measurement parameters were selected based on pre-heat plateau tests and dose recovery tests. Table 2 shows the used SAR procedure. In the SAR procedure, the natural OSL signal ($L_n$) of an aliquot is compared to the regenerated OSL signal ($L_i$) induced by a beta dose from the calibrated source. Following each measurement of $L_n$ or $L_i$, the OSL response to a fixed beta dose (test dose) is recorded ($T_n$, $T_i$). This measurement serves to monitor luminescence sensitivity changes during the measurement procedure. A range of regenerative beta doses is used, including a zero dose and a repeat point, and OSL responses are used to construct a sensitivity-corrected dose response curve ($L_i/T_n$ data fitted with Equation (2)):

$$\frac{L_i}{T_i} = L_s \cdot \left(1 - \exp\left(-\frac{D}{D_0}\right)\right) + cD \quad (2)$$

In this equation, $L_i/T_i$ is the sensitivity-corrected luminescence signal and $L_s$ is the normalized saturation level of the exponential function, obtained from the fit. D is the absorbed dose (expressed in Gy, with 1 Gy equal to 1 J of absorbed energy per kg material). For each of the regenerative dose points, D is known from the duration of beta radiation in combination with the source calibration. $D_0$ (Gy) is a shape parameter indicative of the onset of saturation, and c is a constant. By projecting the sensitivity corrected natural OSL signal ($L_n/T_n$) on this dose response curve, a measure of the equivalent dose is obtained for the aliquot. Fig. 3 shows examples of an OSL decay curve and an OSL dose response curve.

A number of criteria were used to accept only results for aliquots with suitable luminescence characteristics. Data was rejected if: 1) The fit of the dose response curve with equation (2) produced a negative constant c. 2) There were indications for feldspar contamination: significant IR test dose response (>20% of the (post-IR) blue response) in combination with more than 10% depletion of the (post-IR) blue test dose response due to IR exposure. 3) The sensitivity correction failed: recycling ratio outside the 0.9–1.1 range.

To obtain statistically meaningful results, measurements were repeated on at least 21 aliquots for each sample.

The palaeodose (Gy) was determined from the equivalent dose distribution. Often the Central Age Model (CAM, Galbraith et al., 1999) is used for this, but recent publications suggest this may induce a systematic underestimation, as it is based on the geometric rather than arithmetic mean (Guérin et al., 2017). Therefore, we adopted a simple unweighted mean, after iterative removal of outliers (equivalent dose estimates deviating more than 2 standard deviations from the sample mean). The thus obtained palaeodose was the best estimate of burial dose.

### 2.4.4. Dose rate estimation

To translate the burial dose estimate into a deposition age, we also needed to quantify the ionizing dose absorbed by the mineral grains each year. Towards this dose rate estimation, the specific activities of $^{40}$K and several radionuclides in the Uranium ($^{234}$Th, $^{214}$Pb, $^{214}$Bi, $^{210}$Pb) and Thorium ($^{228}$Ac, $^{212}$Pb, $^{212}$Bi) decay chains were measured using a gamma-spectrometer. The bulk samples were first dried at 100 °C for water content estimation. Subsequently the samples were ashed for 24 h at 500 °C for organic content estimation, homogenized by grinding and finally cast in wax to ensure radon retention.

The measured activities in the obtained wax samples were converted into dose rates as described in detail by Guérin et al., 2011. These 'dry' infinite matrix dose rates were attenuated for organic and water content (Aitken, 1985; Madsen et al., 2005), to take into account the part of radiation that was absorbed by water and organics and did not reach the mineral grains. For water attenuation of the dose rate, measured water contents were used (varying from 8 to 24% by weight), with a minimum of 20% water by weight for all samples below the groundwater table (based on a porosity of about 34% for sand; Weerts, 1996). The organic contents were below 1% by weight for all OSL samples. Attenuation of the dose rate by organics was taken into account by assuming similar absorption by water and organics (Madsen et al., 2005). A contribution of cosmic rays attenuated for depth was included in the total dose rate as well (Prescott and Hutton, 1994). Given the dependence of cosmic dose rate on burial depth, an assumption on burial history was needed. Based on preliminary dating results, immediate burial to present depth for all samples younger than 65 ka OSL age was assumed, and gradual burial for older samples. Grain-size attenuation was applied to the beta-dose rate (Mejdahl, 1979), to take into account shielding effects of the grain itself, and finally a small contribution of internal alpha radiation was assumed (Vandenberghe et al., 2008).

### 2.4.5. OSL age determination

OSL ages are determined by dividing the sample palaeodose by the sample dose rate. The burial age of the sample is then provided by the age equation:

$$Age(ka) = \frac{\text{Palaeodose (Gy)}}{\text{Dose rate (Gy/ka)}} \quad (3)$$

Systematic and random errors in both palaeodose and dose rate were taken into account and incorporated in the uncertainty of the reported OSL age. Ages are reported in thousands of calendar years (ka) before sampling (reference year 2009 CE).

### 2.4.6. Validity check for obtained OSL ages

One of the basic assumptions for valid OSL dates is that the signal must have been reset prior to deposition and burial. Incomplete resetting would result in a remaining latent OSL signal upon burial and, if unaccounted for, would result in overestimation of the burial age. This phenomenon is referred to as poor bleaching, or heterogeneous bleaching (e.g. Wallinga et al., 2002). For samples of Holocene age, heterogeneous bleaching is quite easily detected based on the equivalent dose distribution (e.g. Bailey and Arnold, 2006). In such cases an estimate of the burial age can be obtained using e.g. the Minimum Age Model (MAM; Galbraith et al., 1999) provided that aliquots are small

enough. For Pleistocene samples, such as in this Eerbeek case study, identification of poor bleaching is more challenging, and application of the MAM may lead to age underestimation (Thomsen et al., 2005).

In the present study three approaches were combined to identify samples with poor bleaching and overestimation of the age. Each of the methods assigns penalty points to a sample to indicate whether or not it may have been affected by poor bleaching.

Firstly, samples that provided inconsistent chronologies in relation to underlying samples were identified. A deviation from stratigraphic order may provide evidence for poor bleaching, although there can be other causes as well (e.g. related to errors in dose rate estimation). Each sample was assigned penalty points for potential problems: 1) No penalty was assigned if the sample provided an OSL age which was stratigraphically consistent. 2) One point was assigned if the sample was older than one or more samples obtained below, but OSL ages agreed within 1-sigma (unshared error only; see Rhodes et al., 2003). 3) Four points were assigned if the OSL age was older than one or more underlying samples taking into account 1-sigma uncertainties in OSL ages of both samples (unshared error only).

Secondly, samples were identified for which burial age estimates were strongly dependent on the 'age model' used to obtain the palaeodose from the equivalent dose distribution. For heterogeneously bleached samples with wide equivalent dose distributions (e.g. Duller, 2008), the minimum age model (MAM; Galbraith et al., 1999) was expected to give a much younger result than the unweighted mean procedure adopted for age estimation in this study. Application of the MAM model may be complicated for the age range of interest here, as the overdispersion has been shown to depend on the absorbed dose, likely due to grain-to-grain differences in dose response curve shape (Thomsen et al., 2005). Nevertheless, a large difference between MAM and unweighted mean dose estimates may provide an indication that the burial dose estimate was affected by heterogeneous bleaching (Chamberlain and Wallinga, 2019). The MAM requires input with regard to expected scatter in absence of poor bleaching (sigma-b), and Cunningham and Wallinga (2012) proposed a bootstrapping approach to take into account uncertainty in this sigma-b estimate. Here, we obtained an estimate of sigma-b from the overdispersion obtained on the samples using the Central Age Model (Galbraith et al., 1999). If we assume that part of our samples was well bleached, the lower overdispersion estimates provided the sigma-b required by the bootstrapped MAM (Chamberlain et al., 2018a, 2018b). We obtained this value by applying the bootstrapped MAM model (with sigma b set to 0) to the overdispersion dataset; the resulting estimate of overdispersion was used as input for our bootstrapped MAM. Then the next step was to compare MAM ages with those obtained through our unweighted mean; the relative difference between both (expressed as % of the adopted OSL age) was expected to be large if the OSL age was affected by heterogeneous bleaching. Again, we assigned penalty points to samples with potential problems: 1) No penalty was assigned for age differences of less than 10%. 2) One point was assigned for age differences between 10 and 20%. 3) Two points were assigned when the difference was greater than 20%.

Thirdly, equivalent-dose estimates obtained on luminescence signals with different light-sensitivity were compared to identify potential poor bleaching. This approach may identify samples that were deposited with little light exposure, even in the unlikely event that light exposure of all grains was of similar duration. The fast-component OSL of quartz (targeted for dating) is much more rapidly reset than feldspar infrared stimulated luminescence (IRSL) signals. Further information can be obtained by comparing IRSL equivalent doses with those obtained by even harder to bleach post-infrared IRSL (pIRIR) and thermoluminescence (TL) signals. Here the approach of Reimann et al. (2016) was adopted to measure multiple signals on poly-mineral samples to identify the degree of bleaching. Eight aliquots were measured for each sample, and mean equivalent dose ratios of IR25/OSL and pIRIR155/IR25, pIRIR255/IR25, TL/IR25 were used as metric for the degree of bleaching. For each of these ratios, the average of all samples was calculated,

**Table 3**
Stratigraphic description of the cores Eerbeek-I and Eerbeek-II to 12 m depth below surface level.

| Unit | Core Eerbeek-I | Unit | Core Eerbeek-II |
|---|---|---|---|
| 1 | Depth: 0.0–0.9 m | 1 | Depth: 0.0–1.6 m |
| 1a | Top; 0.0–0.25 m: Greyish-black organic layer rich in gravel. Ploughed. | 1a | Top: 0.0–0.35 m: Recent, organic material. Fine sands, gravels (up to 2.0 cm). Soil formation (yellow-brown colour). |
| | | 1a | 0.35–0.8 m: Fine sands with occasional small gravel (1 cm). Paleosoil in sediments between 0.3 and 0.8 m (organic A-horizon culminating in brownish-red B-horizon). |
| 1b | 0.25–0.9 m. Badly sorted mixture of sands and subangular gravel (2.5 cm size). Recent soil formation processes (yellow-brown colour). | 1b | 0.8–1.6 m: First fine and sorted sands, then increasingly larger subrounded and rounded gravels (up to 6 cm) and sands with varying grain sizes. |
| **2** | **Depth: 0.9 m - 2.65 m** | **2** | **Depth: 1.6 m - 3.0 m** |
| 2a | 0.9–1.55 m: Well sorted, very fine to moderately fine grey sands. No organic layers. | 2a | 1.6–1.8 m: Loam layer with organic matter. |
| | | 2a | 1.8–2.85 m: Moderately fine to moderately coarse grey sand with a few larger grains. Thin laminae of peat. Cross-bedding present. |
| 2b | 1.55–2.65: Massive, moderately compacted, black peat deposit. | 2b | 2.85–3.0 m: Organic-rich, peat material, mixed with moderately fine to moderately coarse grey sand. |
| **3** | **Depth: 2.65–3.2 m** | **3** | **Depth: 3.0–3.5 m** |
| | 2.7–3.2 m: Badly sorted fine to extremely coarse sands and sub rounded to subangular gravels (quartz clasts up to 1.2 cm). | | 3.0–3.5 m: Moderately to extremely coarse sands. Gravels (up to 0.6 cm). No organic matter. |
| **4** | **Depth: 3.2–7.6 m** | **4** | **Depth: 3.5–5.3 m** |
| 4a | 3.2–3.7 m: 5- to 10-cm thick, loamy, brown strata with organic material interbedded with medium to coarse sands with some small (2–3 mm) gravels. Indications of cryoturbation. | 4a | 3.5–3.8 m: Moderately fine to moderately coarse sand rich in organic material. |
| 4a | 3.7–4.0 m: Fine to moderately fine sands with oxidation-reduction spots and some loam. | 4a | 3.8–4.3 m: Black to brown peat layer with decreasing black organic matter and increasing fine sands with increasing depth. |
| 4a | 4.0–4.3 m: Fine sand layer with high clay content and some peaty and other organic material. | | |
| 4b | 4.3–5.25 m: Very fine to moderately fine sands with high loam and clay content. Occasional laminae of black organic material (less prevalent compared to 4a). Alternating brown oxidation/reduction spots. | 4b | 4.3–5.1 m: Very fine to moderately fine sands. Intercalations of moderately fine to moderately coarse sands and thin, brown loam and clay laminae. |
| 4b | 5.25–7.25 m: Well sorted, fine to medium, grey sands with planar cross bedding. | 4b | 5.1–5.3 m: Brownish-grey, moderately fine to moderately coarse sands. |
| 4b | 7.25–7.6 m: Grey, medium fine to medium course, relatively well sorted sands. A few subrounded quartz gravel clasts present in the upper section. | 4b | At 5.3 m: a gravel bank. |
| **5** | **Depth: 7.6–8.0 m** | | **(No further sampling possible)** |
| | 7.6-8.0: Badly sorted medium to extremely course sands and gravels. Rounded and | | |

(*continued on next page*)

**Table 3** (*continued*)

| Unit | Core Eerbeek-I | Unit | Core Eerbeek-II |
|---|---|---|---|
| | subrounded gravels up to 1 cm diameter. | | |
| 6 | **Depth: 8.0–12.0 m** 8.0–12.0 m: Up to 1-m thick peat layers intercalating with relatively well sorted, medium to coarse sands. Thin laminae of organic matter, silt and clay and also present. | | |
| 7 | **Depth: 12.0–12.3 m** 12.0–12.3 m: Brownish-grey, moderately coarse to extremely coarse, badly sorted sand. Intercalations of small strings of gravel (up to 0.5 cm diameter). | | |

and a penalty point was assigned if a ratio was greater than this mean (taking 1-sigma error tolerance). Hence, between zero and four penalty points could be assigned to each sample with more points indicating a higher likelihood of poor resetting circumstances.

Penalty points assigned in the second and third approach were added together to provide a likelihood of insufficient bleaching, with two points or more interpreted as suspect. Points of all three approaches were summed to provide a validity estimate for the OSL age obtained on the sample, resulting in the following validity estimates: 1) OK; no penalties assigned. 2) Likely OK; one or two penalties assigned. 3) Questionable; more than two penalties assigned. The results in the first two validity categories were expected to provide robust geochronological data and were used for stratigraphic interpretation and for comparison with $^{14}$C ages.

## 3. Results

### 3.1. Stratigraphy

A summary description of the lithology and sedimentary structures of the two Eerbeek cores is given in Table 3, and shown in Fig. 4. These descriptions were made through visual and tactile inspection of differences in grain size and colour and description of sedimentary structures.

Based on the descriptions we identify 7 main stratigraphic units with subdivisions The upper unit (1) consists of intercalated deposits of loam, peat and sand including a gravelly sand layer, with evidence of soil formation and ploughing disturbance near the top. Unit 2 is again intercalations of loam, peat and fine sands. Unit 3 contains (coarse) sand and gravels. Below this layer unit 4 continues with fine sands and organic and peat layers. This unit extends down to 7.6 m in Eerbeek I. Units 5–7 are only encountered in Eerbeek-I, as Eerbeek-II does not

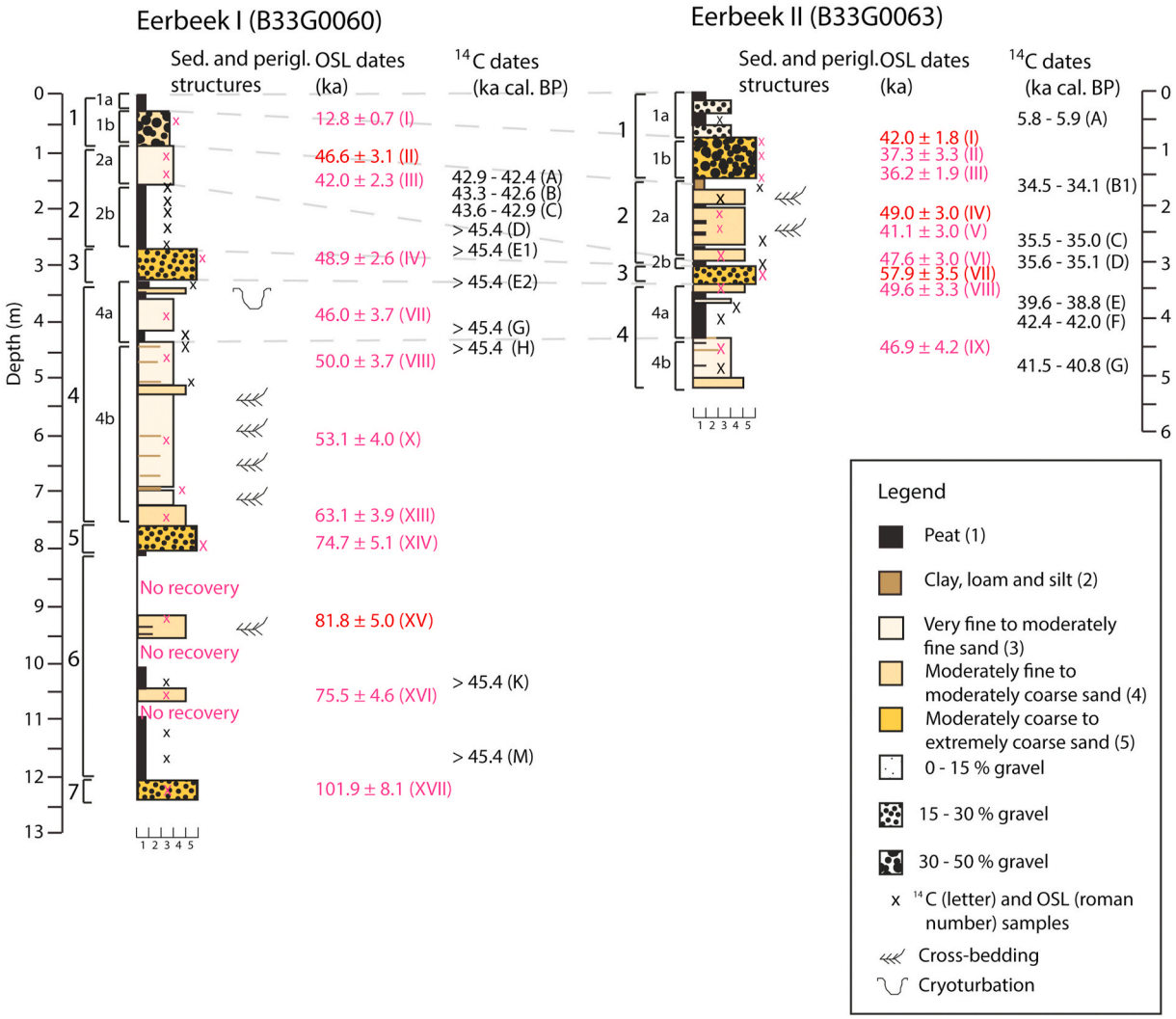


**Fig. 4.** Schematized representation of the lithology and sedimentological features for the two cores Eerbeek-I and Eerbeek-II, together with $^{14}$C and OSL results. The OSL results validated as questionable (section 3.3) are marked in red colour.

**Table 4**
$^{14}$C dating results for Eerbeek-I and Eerbeek-II (sub)samples.

| Sample name | Depth (m) | Lab ID | $^{14}$C age (ka BP) | Age (ka calBP, 1σ range) |
|---|---|---|---|---|
| Eerbeek-I | | | | |
| Eerbeek I A | 1.51 | GrA-52109 | 23.7 ± 0.1 | |
| Eerbeek I A+ | | GrA-57983 | 38.7 ± 0.4 | 42.9–42.4 |
| Eerbeek I B | 1.75 | GrA-52110 | 39.1 ± 0.5 | 43.3–42.6 |
| Eerbeek I C | 2.06 | GrA-52111 | 27.5 ± 0.1 | |
| Eerbeek I C+ | | GrA-57984 | 39.6 ± 0.4 | 43.6–42.9 |
| Eerbeek I C wood | | GrA-52112 | 1.72 ± 0.04 | |
| Eerbeek I D | 2.36 | GrA-52113 | 43.7 ± 0.8 | |
| Eerbeek I D+ | | GrA-57985 | 50.8 ± 2.6 | >45.4 |
| Eerbeek I E1 | 2.62 | GrA-52114 | 49.9 ± 2.2 | >45.4 |
| Eerbeek I E2 | 3.27 | GrA-52116 | 46.5 ± 1.2 | >45.4 |
| Eerbeek I G | 4.11 | GrA-52121 | 51.7 ± 4.0 | >45.4 |
| Eerbeek I H seed | 4.23 | GrA-49442 | 47.9 ± 2.0 | |
| Eerbeek I H | | GrA-48932 | 37.2 ± 0.3 | |
| Eerbeek I H+ | | GrA-57987 | 52.5 ± 2.5 | >45.4 |
| Eerbeek I K | 10.43 | GrA-48933 | 62.9 ± 5.6 | >45.4 |
| Eerbeek I M | 11.60 | GrA-49246 | 58.4 ± 2.7 | >45.4 |
| **Eerbeek-II** | | | | |
| Eerbeek II A | 0.51 | GrA-48936 | 5.1 ± 0.04 | 5.9–5.8 |
| Eerbeek II B1 | 1.68 | GrA-52570 | 29.1 ± 0.2 | |
| Eerbeek II B1+ | | GrA-57990 | 30.3 ± 0.2 | 34.5–34.1 |
| Eerbeek II C | 2.63 | GrA-52120 | 29.3 ± 0.2 | |
| Eerbeek II C+ | | GrA-57992 | 31.4 ± 0.2 | 35.5–35.0 |
| Eerbeek II D | 2.96 | GrA-48937 | 29.8 ± 0.2 | |
| Eerbeek II D+ | | GrA-57993 | 31.5 ± 0.2 | 35.6–35.1 |
| Eerbeek II E | 3.79 | GrA-52119 | 32.9 ± 0.2 | |
| Eerbeek II E+ | | GrA-57994 | 34.7 ± 0.3 | 39.6–38.8 |
| Eerbeek II F | 4.00 | GrA-48938 | 34.8 ± 0.2 | |
| Eerbeek II F+ | | GrA-57995 | 36.8 ± 0.3 | |
| Eerbeek II F++ | | GrA-58445 | 37.9 ± 0.3 | 42.4–42.0 |
| Eerbeek II G | 4.87 | GrA-52572 | 34.8 ± 0.3 | |
| Eerbeek II G+ | | GrA-57996 | 36.5 ± 0.3 | 41.5–40.8 |

reach below unit 4 till only 5.3 m. The original CPT results on both locations indicate that these 7 main stratigraphic units are present in large parts of the fan area, providing some confidence that layer boundaries can be expected to represent levels of similar age. Hence we use this specific stratigraphic information as an indicative verification tool to compare the OSL and $^{14}$C dating results in both cores.

### 3.2. $^{14}$C results

The $^{14}$C dating results of the selected and pre-treated plant remains from each deposit sample are shown in Table 4 and Fig. 4. The description '+' or '++' in the sample name refers to the applied additional chemical pre-treatments, as described in Table 1. A general description of the selected organic material from the samples and their relative amount are given in Appendix A (Table A.1. and Table A.2). In Appendix B examples of selected and pre-treated plants remains for (part of) the investigated samples are shown. The measured percentage carbon, $\delta^{13}$C value (IRMS) and F$^{14}$C values (in %) of each organic sample are shown in Appendix C (Table C.1).

The dating limit of the $^{14}$C method is calculated from the average measured $^{14}$C background level and its 2-sigma uncertainty, following the conventions as introduced by Olsson (1989). In this study the average non-background corrected F$^{14}$C value for $^{14}$C-free anthracite was 0.28 ± 0.11% (n = 26; obtained from 6 different AMS batches in which also Eerbeek samples were measured). Based on these values we set the detection limit to F$^{14}$C = 0.28% + 2 × 0.11% = 0.50%, corresponding to a $^{14}$C age of 42.6 ka BP. After calibration to calendar years (using Oxcal 4.3 and calibration curve IntCal13) this yielded an age limit of approximately 45.4 ka calBP.

Given the $^{14}$C detection limit of 45.4 ka calBP and considering only the result of the most extensively applied chemical pre-treatment method for the particular sample material, samples Eerbeek-I A to C and all Eerbeek-II samples have finite ages, and Eerbeek-I D to M have infinite ages. Although the results of both Eerbeek-I and Eerbeek-II cores demonstrate stratigraphic consistency, the ages of organic deposits at the same depth for the uppermost 5 m differ approximately 9 ka between both cores.

### 3.3. OSL results

Dose rate activity concentrations obtained for different radionuclides from the $^{238}$U series (Table 5) agreed well and showed no indications for disequilibrium. $^{210}$Pb activity concentrations were on average 17% lower than those for $^{214}$Pb and $^{214}$Bi, indicating a Rn escape of 17%, which is in line with expectations. Dose rates ranged from 0.58 ± 0.02 to 2.19 ± 0.10 Gy/ka for the prepared quartz fraction, with an average of 1.14 Gy/ka. Variations can be explained from differences in lithology and source material.

The SAR method adopted for equivalent-dose estimation was tested using a dose-recovery test, in which samples were bleached, and then received a known laboratory dose that was measured as an unknown. The test was performed on all samples, and indicated that a laboratory dose could be accurately determined using the adopted measurement procedures. See Fig. 5 (dose recovery ratio: 0.97 ± 0.01, n = 79, overdispersion obtained through the Central Age Model 10%).

The overall results of the OSL age validity verification (according to the method described in section 2.4.6) are shown in Table 6. Three samples showed evidence of poor bleaching: Eerbeek-I sample 'NCL-8211056' and Eerbeek-II samples 'NCL-8311064' and 'NCL-8311066'. From these samples, the dating results of 'NCL-831164' were also stratigraphically inconsistent, and total validity was judged questionable based on the number of penalty points.

For Eerbeek-I samples NCL-8211051 and NCL-821158 and Eerbeek-II samples NCL-8311129 and NCL-83111062 stratigraphically inconsistent results were obtained, even though there were no clear signs of incomplete bleaching. Reasons for this inconsistency remain unclear, although we suspect that problems may be related to dose-rate estimation in these heterogeneous deposits (see e.g. Wallinga and Bos, 2010).

An overview of the OSL dating results is shown in Table 7 and Fig. 4. The validity was judged questionable for 5 out of 21 samples (these are marked grey in Table 7). The remaining dataset (16 samples) provides a highly consistent and likely robust chronological framework, which allows comparison with $^{14}$C results.

The OSL ages of Eerbeek-I and Eerbeek-II indicate a slightly different age-depth profile between both cores for the upper 2.5 m below the surface and similarity below 2.5 m depth.

## 4. Discussion

### 4.1. Combining stratigraphic, $^{14}$C and OSL evidence

Fig. 4 provides an overview of the core stratigraphy and dating results. Here we first compare OSL and $^{14}$C results, and then use a stratigraphic correlation of the cores to discuss inconsistencies in dating results.

The OSL and $^{14}$C dating results are shown together in Fig. 6. The results of Eerbeek-I agree very well and form a consistent age-depth pattern (Fig. 6, upper part). Finite $^{14}$C ages were only obtained for the upper three dated samples above 2.1 m depth. All three results are close to the detection limit of 45.4 ka calBP, but agree favourably with the OSL constraints for the specific peat layer (located at 2.65–1.55 m depth), indicating that it developed between 48.8 ± 2.6 ka and 41.9 ±

**Table 5**
Dose rate estimates.

| Sample code | | Depth | Water content (weight %) | Org. content (weight %) | Radionuclide concentrations (Bq/kg) | | | Attenuated dose rates (Gy/ka) | | | |
|---|---|---|---|---|---|---|---|---|---|---|---|
| NCL | Sample name | (m) | | | $^{238}$U | $^{232}$Th | $^{40}$K | Beta | Gamma | Cosmic | Total |
| Eerbeek I | | | | | | | | | | | |
| NCL-8211127 | Eerbeek I - I | 0.44 | 20.0 ± 5.0 | 0.28 ± 0.03 | 13.12 ± 0.12 | 12.04 ± 0.25 | 263 ± 3 | 0.64 ± 0.04 | 0.36 ± 0.02 | 0.25 ± 0.01 | 1.26 ± 0.05 |
| NCL-8211051 | Eerbeek I - II | 1.04 | 10.3 ± 2.6 | 0.44 ± 0.04 | 12.76 ± 0.15 | 12.44 ± 0.34 | 254 ± 3 | 0.69 ± 0.03 | 0.40 ± 0.02 | 0.19 ± 0.01 | 1.29 ± 0.04 |
| NCL-8211052 | Eerbeek I - III | 1.34 | 13.1 ± 3.3 | 0.37 ± 0.04 | 10.76 ± 0.30 | 9.66 ± 0.21 | 249 ± 5 | 0.62 ± 0.03 | 0.33 ± 0.02 | 0.19 ± 0.01 | 1.15 ± 0.04 |
| NCL-8211053 | Eerbeek I - IV | 2.86 | 12.8 ± 3.2 | 0.22 ± 0.02 | 6.90 ± 0.20 | 6.08 ± 0.22 | 166 ± 4 | 0.42 ± 0.02 | 0.23 ± 0.01 | 0.15 ± 0.01 | 0.81 ± 0.03 |
| NCL-8211054 | Eerbeek I - VII | 3.85 | 21.7 ± 5.4 | 0.58 ± 0.06 | 23.42 ± 0.22 | 22.86 ± 0.50 | 388 ± 4 | 0.98 ± 0.07 | 0.60 ± 0.03 | 0.13 ± 0.01 | 1.72 ± 0.07 |
| NCL-8211055 | Eerbeek I - VIII | 4.51 | 24.0 ± 6.0 | 0.70 ± 0.07 | 21.87 ± 0.19 | 23.03 ± 0.43 | 434 ± 4 | 1.03 ± 0.07 | 0.62 ± 0.03 | 0.12 ± 0.01 | 1.79 ± 0.08 |
| NCL-8211056 | Eerbeek I - X | 6 | 21.4 ± 5.4 | 0.31 ± 0.03 | 15.15 ± 0.14 | 15.47 ± 0.33 | 389 ± 3 | 0.89 ± 0.06 | 0.49 ± 0.03 | 0.10 ± 0.01 | 1.49 ± 0.07 |
| NCL-8211057 | Eerbeek I - XIII | 7.5 | 20.0 ± 5.0 | 0.12 ± 0.01 | 6.36 ± 0.14 | 5.84 ± 0.19 | 154 ± 4 | 0.35 ± 0.02 | 0.18 ± 0.01 | 0.09 ± 0.00 | 0.63 ± 0.03 |
| NCL-8211128 | Eerbeek I - XIV | 7.92 | 20.0 ± 5.0 | 0.65 ± 0.07 | 8.73 ± 0.32 | 7.96 ± 0.16 | 162 ± 4 | 0.40 ± 0.03 | 0.23 ± 0.01 | 0.14 ± 0.01 | 0.79 ± 0.03 |
| NCL-8211058 | Eerbeek I - XV | 9.14 | 20.0 ± 5.0 | 0.33 ± 0.03 | 5.96 ± 0.26 | 5.26 ± 0.14 | 183 ± 4 | 0.40 ± 0.03 | 0.20 ± 0.01 | 0.14 ± 0.01 | 0.76 ± 0.03 |
| NCL-8211059 | Eerbeek I - XVI | 10.46 | 20.0 ± 5.0 | 0.16 ± 0.02 | 4.77 ± 0.17 | 3.90 ± 0.13 | 133 ± 4 | 0.29 ± 0.02 | 0.15 ± 0.01 | 0.13 ± 0.01 | 0.58 ± 0.02 |
| NCL-8211060 | Eerbeek I - XVII | 12.25 | 21.7 ± 5.4 | 0.94 ± 0.09 | 9.11 ± 0.15 | 6.98 ± 0.22 | 224 ± 3 | 0.50 ± 0.03 | 0.25 ± 0.01 | 0.12 ± 0.01 | 0.88 ± 0.04 |
| **Eerbeek II** | | | | | | | | | | | |
| NCL-8311129 | Eerbeek II - I | 0.84 | 12.1 ± 3.0 | 0.65 ± 0.07 | 9.50 ± 0.14 | 9.62 ± 0.17 | 178 ± 3 | 0.48 ± 0.03 | 0.28 ± 0.01 | 0.20 ± 0.01 | 0.97 ± 0.03 |
| NCL-8311130 | Eerbeek II - II | 1.07 | 8.2 ± 2.1 | 0.45 ± 0.04 | 13.96 ± 0.13 | 13.91 ± 0.31 | 231 ± 2 | 0.68 ± 0.03 | 0.42 ± 0.02 | 0.19 ± 0.01 | 1.29 ± 0.04 |
| NCL-8311061 | Eerbeek II - III | 1.47 | 14.7 ± 3.7 | 0.50 ± 0.05 | 16.26 ± 0.17 | 15.30 ± 0.45 | 253 ± 4 | 0.71 ± 0.04 | 0.45 ± 0.02 | 0.19 ± 0.01 | 1.36 ± 0.05 |
| NCL-8311062 | Eerbeek II - IV | 2.12 | 17.5 ± 4.4 | 0.18 ± 0.02 | 6.17 ± 0.13 | 5.60 ± 0.11 | 190 ± 3 | 0.43 ± 0.03 | 0.21 ± 0.01 | 0.16 ± 0.01 | 0.82 ± 0.03 |
| NCL-8311131 | Eerbeek II - V | 2.37 | 15.2 ± 3.8 | 0.13 ± 0.01 | 5.19 ± 0.19 | 4.69 ± 0.12 | 214 ± 3 | 0.47 ± 0.03 | 0.22 ± 0.01 | 0.16 ± 0.01 | 0.86 ± 0.03 |
| NCL-8311063 | Eerbeek II - VI | 2.82 | 20.0 ± 5.0 | 0.73 ± 0.07 | 7.14 ± 0.25 | 6.50 ± 0.26 | 175 ± 4 | 0.40 ± 0.03 | 0.21 ± 0.01 | 0.15 ± 0.01 | 0.76 ± 0.03 |
| NCL-8311064 | Eerbeek II - VII | 3.35 | 20.0 ± 5.0 | 0.19 ± 0.02 | 6.93 ± 0.20 | 6.19 ± 0.19 | 155 ± 4 | 0.37 ± 0.03 | 0.20 ± 0.01 | 0.14 ± 0.01 | 0.72 ± 0.03 |
| NCL-8311065 | Eerbeek II - VIII | 3.58 | 22.5 ± 5.6 | 0.71 ± 0.07 | 22.41 ± 0.25 | 22.37 ± 0.39 | 460 ± 6 | 1.09 ± 0.08 | 0.63 ± 0.03 | 0.14 ± 0.01 | 1.86 ± 0.08 |
| NCL-8311066 | Eerbeek II - IX | 4.46 | 23.3 ± 5.8 | 0.70 ± 0.07 | 29.16 ± 0.25 | 29.85 ± 0.53 | 494 ± 6 | 1.24 ± 0.09 | 0.78 ± 0.04 | 0.12 ± 0.01 | 2.16 ± 0.10 |

2.3 ka. For the lower part of this same peat layer, two infinite $^{14}$C ages are obtained (e.g. > 45.4 ka calBP). Also these results are in agreement with the obtained OSL ages. Five additional $^{14}$C samples from deeper parts all returned infinite ages as well.

The $^{14}$C dating results of Eerbeek-II (Fig. 6, lower part) follow a different age-depth pattern than the OSL results. The pattern appears shifted in age or depth below 2 m depth. All dated $^{14}$C samples returned finite ages and all dates are younger compared to the OSL results.

Because the true ages of the deposits are not known and these cannot be identified based on the two independent $^{14}$C and OSL datasets alone, additional information about the core stratigraphy and chronology (section 3.1) is needed to identify which dated chronology is most likely to be correct. Based on the lithology of the two cores it is expected that the ages in both cores are similar at the major depositional unit boundaries around 3 m depth (unit 2–3 and unit 3–4 transitions). This similarity between the cores is indeed visible for the OSL dates: OSL dating constrains the unit 2–3 transition between 42-49 ka and 48–50 ka for Eerbeek-I and Eerbeek-II respectively and the unit 3–4 transition between 49-50 ka and 48–50 ka. For $^{14}$C dating, both transitions are dated older than 45.4 ka cal BP for Eerbeek I, while for Eerbeek-II these transitions date between 35 and 39 ka cal BP. Because the $^{14}$C dates of Eerbeek-I fit with those obtained by OSL and the OSL results fit with the stratigraphic interpretation, the measured $^{14}$C results of Eerbeek-II below unit 2 are very likely too young. Based on comparison with the OSL dates alone, the $^{14}$C results of Eerbeek-II likely underestimate the age of all deposits below unit 1 (see Fig. 4).

The alternative scenario, in which the anomaly observed in the results of Eerbeek-II is attributed to overestimation of the OSL ages, seems unlikely. Two independent methods to check for incomplete and heterogeneous resetting were applied, and suspicious OSL samples were rejected (Table 7). In addition, as explained above, the stratigraphy for both cores shows similarities in depositional boundary units and the OSL dates of both cores are consistent with that profile. An unlikely large shift of several meters in the depth of these boundary units would be necessary to match the younger $^{14}$C dates of Eerbeek-II.

Hence, the Eerbeek-I $^{14}$C results and Eerbeek-I and Eerbeek-II OSL results are likely to be accurate, while the Eerbeek-II $^{14}$C ages appear underestimated (too young).

### 4.2. Potential reasons for $^{14}$C age underestimation

Underestimation of $^{14}$C ages was not only observed for the Eerbeek-II samples, but initially also in the Eerbeek-I samples after chemical pre-treatment with the 'light' ABA method (Table 1). For both cores, the results of different multiple measured subsamples (Table 4, column with $^{14}$C ages) very clearly show two of the different challenging factors when dating sediments >30 ka calBP based on $^{14}$C measurements of plant remains. This has also been observed by Briant and Bateman (2009), and was further discussed in Briant et al. (2018).

A first challenge is identification of plant remains that have intruded (possibly long) after deposition of the original plant remains. Tree roots grow meters below the surface level and could potentially alter the organic composition of a deposit. The piece of wood in sample 'Eerbeek-I C' (GrA-52112) was very young, and therefore likely a piece of a tree root, even though it could not be directly (based on visual inspection) identified as a foreign piece of organic material prior to $^{14}$C dating. This stresses the importance of biological determination of species in the organic sample after chemical pre-treatment and selection of single or specific mixed species prior to $^{14}$C dating. Briant et al. (2018) also pointed this out. When feasible, a selection of plant materials that were most likely part of the original deposit (such as leaves or seeds) should be made. There are no indications of differences between both cores in the age-diversity (heterogeneity) of the plant remains that were selected and which could explain the too young dates of the Eerbeek-II deposits. Similarities were found between both cores in the composition of the selected materials (although not identified for species specifically), in the type of seeds present (based on similar shapes) and the presence of mica (indication for similarities in deposit origin) below a similar depth (see also Appendices A and B).

A second challenge is how to thoroughly remove foreign carbon molecules by chemical pre-treatment without losing too much original organic sample material for reliable dating. This issue is well investigated and discussed by Briant et al. (2018), who reviewed and discussed the use of different chemical pre-treatment methods (beside mild and

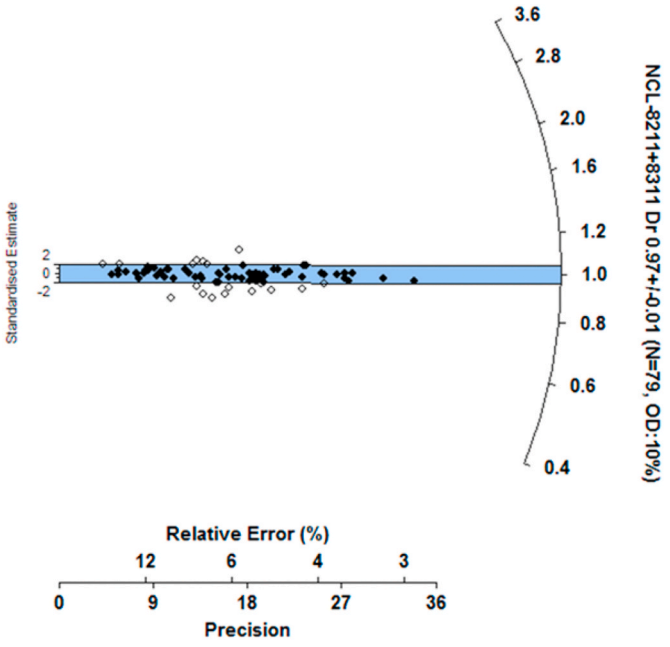


**Fig. 5.** Results dose recovery test.

strong ABA, also ABOx, ABA-bleach and some other methods) and shows that the options for an effective and harsh pre-treatment are very limited. In our current study, older $^{14}$C ages (Table 4) were obtained after a second or even third chemical pre-treatment, using higher temperatures and higher concentration of alkaline solution (Table 1; analogue to 'strong ABA' methods as mentioned in Briant et al., 2018).

The approximate $^{14}$C ages of the removed organic material after the second ('mild') and third ('strong') pre-treatments and the mass loss after each treatment are shown in Table 8. The ages of the dissolved and removed carbon fractions are calculated based on the measured $^{14}$C values before and after a pre-treatment and the measured %C (both shown in Appendix C) and the fractions of mass loss. The combination of age and carbon fraction of both original carbon material and the (in this case) younger carbon fractions determine the age of the dissolved carbon fraction. After the second ('mild') alkaline pre-treatment, with higher concentration and temperature compared to the first alkaline pre-treatment, approximately 25% of the sample mass was lost and the age of removed fraction was relatively young compared to the remaining material. This stresses the importance of applying the alkaline pre-treatment at higher than room temperatures and using alkaline (NaOH or KOH) concentrations of at least 0.2 M, in order to remove added carbon fractions. This confirms the results as obtained by Briant et al. (2018).

After the third ('strong') alkaline pre-treatment of sample 'Eerbeek-II F', applying higher temperature (90 °C), concentration and duration, almost 80% of material was lost and the age of the removed material was relatively closer to the age of the remaining material. Hence, during this third strong pre-treatment a large fraction of original carbon material was dissolved as well, while the effect on the age of the remaining material was not significant anymore. This suggests that an optimum in temperature, concentration and duration of the alkaline pre-treatment should be found for the removal of especially younger carbon while preserving most of the original carbon material. However, since this was the third pre-treatment of the same sample material (it already obtained a 'light' and 'mild' pre-treatment), the results could also indicate that the ability to remove the younger carbon fractions from the sample material, either by using a strong alkaline solution or also by using other chemicals as described by Briant et al. (2018) such as ABOx or chlorite, is limited. This might be related to the origin of the selected organic fraction, i.e. the humin fraction.

During the humification process organic matter is transformed into humic substances. See Zaccone et al. (2011), who refer to Stevenson (1994): "Humification is a reconstructive process that starts from all the derived molecules occurring in the medium at various stages of decomposition, which are then to some extent reassembled, recombined and re-polymerized to form humic substances, that is humic acids, fulvic acids and humin."

Generally, the purpose of the applied chemical pre-treatments for $^{14}$C dating is that easily transported humic and fulvic acids are dissolved and removed (e.g., Mook and Streurman, 1983), while the humin fraction (which is not easily transported in the soil and therefore the least influenced by foreign carbon) remains. However, if humins can also be formed in deposits by reaction of younger humic substances (fulvic and humic acids) with those of the original deposit, then the $^{14}$C dates of the selected humin fraction can be affected by foreign carbon as well. In such cases, chemically pre-treated organic materials will still be a mixture of carbon molecules from different deposits. The currently applied pre-treatment methods for $^{14}$C dating of deposit material lack the ability to separate humin fractions from different (carbon) origin. The significance of these contaminated humin fractions depend on their relative size in the total humin fraction and their $^{14}$C values. Because the distribution of the humic substances shows spatial and temporal variations and relies on different soil and climatological factors (Zaccone et al., 2011), local differences in humin composition of deposits may also be observed.

One possible explanation for the differences between the $^{14}$C dates of the two Eerbeek cores could be that relatively large fractions of young humic and fulvic acids in the Eerbeek-II core have reacted with humic substances of the older deposits to humins. This would then explain the rejuvenation of the $^{14}$C dates for Eerbeek-II. For the Eerbeek-I samples a second alkaline-acid pre-treatment appeared necessary to remove sufficient young carbon to obtain an age-depth profile matching the OSL profile and yielding infinite ages where expected. In contrast, finite $^{14}$C ages were still obtained for all Eerbeek-II samples. Although strong chemical pre-treatment led to increased ages, results were still finite. It is striking that the remaining underestimation of $^{14}$C ages only occurs at Eerbeek-II, while the Eerbeek-I and Eerbeek-II $^{14}$C samples were chemically pre-treated and measured in exactly the same way and part of these Eerbeek-I and Eerbeek-II samples were (visually) very similar in botanical composition. This rules out contamination in the laboratory with younger carbon of the Eerbeek-II samples. Therefore, it most likely relates to differences in the carbon composition of the organic samples themselves: the selected humin fraction.

At the Eerbeek-I site, a thick peat layer is present at depths between 1.55 and 2.65 m, while Eerbeek-II does not have a peat layer at these depths and the more sandy and gravelly deposits at this site contain few organic remains (Table 3 and Appendix A). Possibly the thick peat layer of Eerbeek-I functioned as a carbon buffer for the percolating young humic substances from the overlying sediments, decreasing its overall influence on the final $^{14}$C dates of deeper samples significantly. Alternatively, differences in soil chemistry between a peat layer and sandy deposits, or differences in local groundwater flows between both sites in time, may also have influenced the distribution of the humic substances in the deposits of both cores and the formation of humins. Such differences may explain why the Eerbeek-II samples seem to contain relatively more young-carbon humins than Eerbeek-I.

We suggest that the too young ages observed in other $^{14}$C-OSL studies with $^{14}$C dates older than 30 ka (e.g. Magee et al., 1995; Briant and

**Table 6**
Analysis of OSL age validity, based on consistency and indications of poor bleaching.

| Sample | | Depth (m) | Overdispersion (%) | OSL age (ka) | | | Assigned 'penalty points' | | | | | Validity |
|---|---|---|---|---|---|---|---|---|---|---|---|---|
| NCL | Sample name | | | Iterated | MAM | % differ. | Bleaching | | | Stratigraphy | Total | |
| | | | | | | | Heterogen. | Poor | Total | | | |
| **Eerbeek-I** | | | | | | | | | | | | |
| NCL-8211127 | Eerbeek I - I | 0.44 | 21.8 ± 3.9 | 12.8 ± 0.7 | 12.0 ± 1.3 | 6% | | | 0 | 0 | 0 | OK |
| NCL-8211051 | Eerbeek I - II | 1.04 | 32.9 ± 4.9 | 46.6 ± 3.1 | 38.1 ± 4.8 | 18% | 1 | | 1 | **4** | **5** | Questionable |
| NCL-8211052 | Eerbeek I - III | 1.34 | 14.8 ± 2.8 | 42.0 ± 2.3 | 41.5 ± 2.2 | 1% | | | 0 | 0 | 0 | OK |
| NCL-8211053 | Eerbeek I - IV | 2.86 | 24.8 ± 3.8 | 48.9 ± 2.6 | 47.9 ± 4.2 | 2% | | | 0 | 1 | 1 | Likely OK |
| NCL-8211054 | Eerbeek I - VII | 3.85 | 29.9 ± 5.7 | 46.0 ± 3.7 | 40.7 ± 6.4 | 12% | 1 | | 1 | 0 | 1 | Likely OK |
| NCL-8211055 | Eerbeek I - VIII | 4.51 | 18.4 ± 4.1 | 50.0 ± 3.7 | 49.0 ± 3.7 | 2% | | 1 | 1 | 0 | 1 | Likely OK |
| NCL-8211056 | Eerbeek I - X | 6 | 29.2 ± 4.9 | 53.1 ± 4.0 | 47.3 ± 6.9 | 11% | 1 | 1 | **2** | 0 | 2 | Likely OK |
| NCL-8211057 | Eerbeek I - XIII | 7.5 | 22.7 ± 2.7 | 63.1 ± 3.9 | 59.1 ± 4.9 | 6% | | | 0 | 0 | 0 | OK |
| NCL-8211128 | Eerbeek I - XIV | 7.92 | 24.4 ± 4.3 | 74.7 ± 5.1 | 71.2 ± 6.6 | 4% | | 1 | 1 | 0 | 1 | Likely OK |
| NCL-8211058 | Eerbeek I - XV | 9.14 | 28.4 ± 3.9 | 81.8 ± 5.0 | 81.8 ± 6.7 | 1% | | 1 | 1 | **4** | **5** | Questionable |
| NCL-8211059 | Eerbeek I - XVI | 10.46 | 23.4 ± 3.4 | 75.5 ± 4.6 | 72.0 ± 6.2 | 5% | | 1 | 1 | 0 | 1 | Likely OK |
| NCL-8211060 | Eerbeek I - XVII | 12.25 | 32.2 ± 5.3 | 101.9 ± 8.1 | 81.7 ± 11.7 | 20% | 1 | | 1 | 0 | 1 | Likely OK |
| NCL-8311129 | Eerbeek II - I | 0.84 | 24.9 ± 3.9 | 42.0 ± 1.8 | 38.5 ± 3.1 | 8% | | 1 | 1 | **4** | **5** | Questionable |
| **Eerbeek-II** | | | | | | | | | | | | |
| NCL-8311130 | Eerbeek II - II | 1.07 | 21.6 ± 5.5 | 37.3 ± 3.3 | 35.5 ± 2.9 | 5% | | 1 | 1 | 1 | 2 | Likely OK |
| NCL-8311061 | Eerbeek II - III | 1.47 | 24.2 ± 4.1 | 36.2 ± 1.9 | 37.3 ± 2.6 | −3% | | | 0 | 0 | 0 | OK |
| NCL-8311062 | Eerbeek II - IV | 2.12 | 20.9 ± 3.6 | 49.0 ± 3.0 | 50.0 ± 3.3 | −2% | | | 0 | 4 | 4 | Questionable |
| NCL-8311131 | Eerbeek II - V | 2.37 | 21.0 ± 5.1 | 41.1 ± 3.0 | 41.3 ± 3.7 | −1% | | | 0 | 0 | 0 | OK |
| NCL-8311063 | Eerbeek II - VI | 2.82 | 21.7 ± 3.6 | 47.6 ± 3.0 | 47.6 ± 3.6 | 0% | | | 0 | 1 | 1 | Likely OK |
| NCL-8311064 | Eerbeek II - VII | 3.35 | 25.2 ± 3.6 | 57.9 ± 3.5 | 56.7 ± 4.5 | 2% | | 2 | **2** | **4** | **6** | Questionable |
| NCL-8311065 | Eerbeek II - VIII | 3.58 | 23.4 ± 4.5 | 49.6 ± 3.3 | 45.8 ± 4.9 | 7% | | 1 | 1 | 1 | 2 | Likely OK |
| NCL-8311066 | Eerbeek II - IX | 4.46 | 37.1 ± 6.1 | 46.9 ± 4.2 | 34.8 ± 6.6 | 26% | 1 | | **2** | 0 | 2 | Likely OK |

Bateman, 2009; Kliem et al., 2013), can also be caused by relatively large humin fractions with younger age. Interestingly, in all these studies the investigated deposits were not from a thick peat layer and no peat layers were present above the investigated deposits. Perhaps this influences the relative amount of younger age humic and fulvic acids percolating towards older deposits and reacting there to humin fractions.

## 5. Recommendations

The core Eerbeek-II shows that selected and $^{14}$C dated humin fractions in several cases may yield rejuvenated dates. We hypothesize these fractions may in part be secondary formed from younger humic substances (long) after deposition. These younger humin fractions cannot be removed in the generally applied chemical pre-treatment methods. The effect on the dating result would be the largest for deposits with a relatively low content of organic material and for samples with low $^{14}$C content (older than ca. 30 ka). Testing of this hypothesis was beyond the scope of this paper.

Given the significance for radiocarbon dating, especially for deposits older than 30 ka with highly permeable sediments we suggest that further research is needed to investigate differences in humic substances between different cores and deposits and their (possible) influence on the $^{14}$C dating results. This requires further $^{14}$C-OSL comparison studies, which also include soil chemistry to analyse humic acids, fulvic acids and humins (for instance by using FTIR measurement techniques). If it is confirmed that humin fractions can indeed be formed in deposits from younger humic substances and these humin fractions are not removed in the currently applied chemical pre-treatment methods, it should be investigated whether it is possible to distinguish and separate these younger humin fractions. Hydrological analysis might help in investigating the influence of percolation differences between different cores. Further research should be done for multiple cores with ages older than 30 ka, with and without peat layers and with both clastic and organic layers suitable to date by both $^{14}$C and OSL.

With such investigations it might be possible to find out why certain cores or deposits can be dated well by radiocarbon and others not, despite strong chemical pre-treatment. The outcome of the research could then also be used to investigate the reliability of dating results from previous studies (especially for dates older than 30 ka).

Our results underscore the importance of the recommendations by Briant et al. (2018), considering (among others) the selection of specific organic material and the application of a strong ABA-method to remove humic and fulvic acids. Previously published $^{14}$C dates of organic materials from deposits should be treated with care, especially when they are older than ca. 35 ka and when they are not verified by independent methods such as OSL. Based on our results, it is also recommended to be aware of the possible influence of younger humin fractions on the $^{14}$C dating result, especially for deposits with little or no organic material in the overlying deposits. And it is recommended to always verify the $^{14}$C dates with OSL dates in cases where both organic and clastic deposits are available.

The procedures applied in this study to identify and reject outliers in the OSL dataset (section 2.4.6), improved the reliability of the obtained chronologies for both investigated cores and are recommended for other OSL studies as well.

## 6. Conclusions

- For $^{14}$C dating of organic deposits it is essential that specific identified organic material is selected. This material should be chemically pre-treated with an alkaline solution at high temperature and high alkaline concentration to remove adequately the younger aged humic and fulvic acids. This improves the reliability of the obtained $^{14}$C dates.
- The validity check procedure that was described and applied in this study to identify and reject outliers in the OSL dating set, proved to be reliable and useful.

**Table 7**
OSL dating results.

| Sample code NCL | Sample name | Depth (m) | Palaeodose (Gy) | Dose rate (Gy/ka) | Age (ka) | Validity |
|---|---|---|---|---|---|---|
| **Eerbeek I** | | | | | | |
| NCL-8211127 | Eerbeek I - I | 0.44 | 16.0 ± 0.6 | 1.26 ± 0.05 | 12.8 ± 0.7 | OK |
| NCL-8211051 | Eerbeek I - II | 1.04 | 60.0 ± 3.6 | 1.29 ± 0.04 | 46.6 ± 3.1 | Questionable |
| NCL-8211052 | Eerbeek I - III | 1.34 | 48.2 ± 2.1 | 1.15 ± 0.04 | 42.0 ± 2.3 | OK |
| NCL-8211053 | Eerbeek I - IV | 2.86 | 39.5 ± 1.6 | 0.81 ± 0.03 | 48.9 ± 2.6 | Likely OK |
| NCL-8211054 | Eerbeek I - VII | 3.85 | 79.3 ± 5.4 | 1.72 ± 0.07 | 46.0 ± 3.7 | Likely OK |
| NCL-8211055 | Eerbeek I - VIII | 4.51 | 89.3 ± 5.2 | 1.79 ± 0.08 | 50.0 ± 3.7 | Likely OK |
| NCL-8211056 | Eerbeek I - X | 6.00 | 79.1 ± 4.8 | 1.49 ± 0.07 | 53.1 ± 4.0 | Likely OK |
| NCL-8211057 | Eerbeek I - XIII | 7.50 | 39.9 ± 1.7 | 0.63 ± 0.03 | 63.1 ± 3.9 | OK |
| NCL-8211128 | Eerbeek I - XIV | 7.92 | 58.7 ± 3.2 | 0.79 ± 0.03 | 74.7 ± 5.1 | Likely OK |
| NCL-8211058 | Eerbeek I - XV | 9.14 | 61.8 ± 2.8 | 0.76 ± 0.03 | 81.8 ± 5.0 | Questionable |
| NCL-8211059 | Eerbeek I - XVI | 10.46 | 43.7 ± 1.9 | 0.58 ± 0.02 | 75.5 ± 4.6 | Likely OK |
| NCL-8211060 | Eerbeek I - XVII | 12.25 | 89.5 ± 6.0 | 0.88 ± 0.04 | 101.9 ± 8.1 | Likely OK |
| **Eerbeek II** | | | | | | |
| NCL-8311129 | Eerbeek II - I | 0.84 | 40.7 ± 1.2 | 0.97 ± 0.03 | 42.0 ± 1.8 | Questionable |
| NCL-8311130 | Eerbeek II - II | 1.07 | 48.3 ± 4.0 | 1.29 ± 0.04 | 37.3 ± 3.3 | Likely OK |
| NCL-8311061 | Eerbeek II - III | 1.47 | 49.3 ± 2.0 | 1.36 ± 0.05 | 36.2 ± 1.9 | OK |
| NCL-8311062 | Eerbeek II - IV | 2.12 | 39.9 ± 1.9 | 0.82 ± 0.03 | 49.0 ± 3.0 | Questionable |
| NCL-8311131 | Eerbeek II - V | 2.37 | 35.3 ± 2.2 | 0.86 ± 0.03 | 41.1 ± 3.0 | OK |
| NCL-8311063 | Eerbeek II - VI | 2.82 | 36.4 ± 1.7 | 0.76 ± 0.03 | 47.6 ± 3.0 | Likely OK |
| NCL-8311064 | Eerbeek II - VII | 3.35 | 41.9 ± 1.8 | 0.72 ± 0.03 | 57.9 ± 3.5 | Questionable |
| NCL-8311065 | Eerbeek II - VIII | 3.58 | 92.3 ± 4.6 | 1.86 ± 0.08 | 49.6 ± 3.3 | Likely OK |
| NCL-8311066 | Eerbeek II - IX | 4.46 | 101.2 ± 7.8 | 2.16 ± 0.10 | 46.9 ± 4.2 | Likely OK |

- The rejuvenation of $^{14}C$ dates in part of one of the cores is possibly caused by a larger humin fraction of younger carbon in the deposits of this core. Separation of this relatively younger humin fraction from the humin fraction of interest is not possible with the current existing pre-treatment methods.
- Further research of humic substances in deposits of different cores is needed to investigate the possible role of younger humin fractions in specific selected dated organic materials. Local differences in soil chemistry, humification, and percolation may influence the $^{14}C$ dating results of organic materials from deposits.

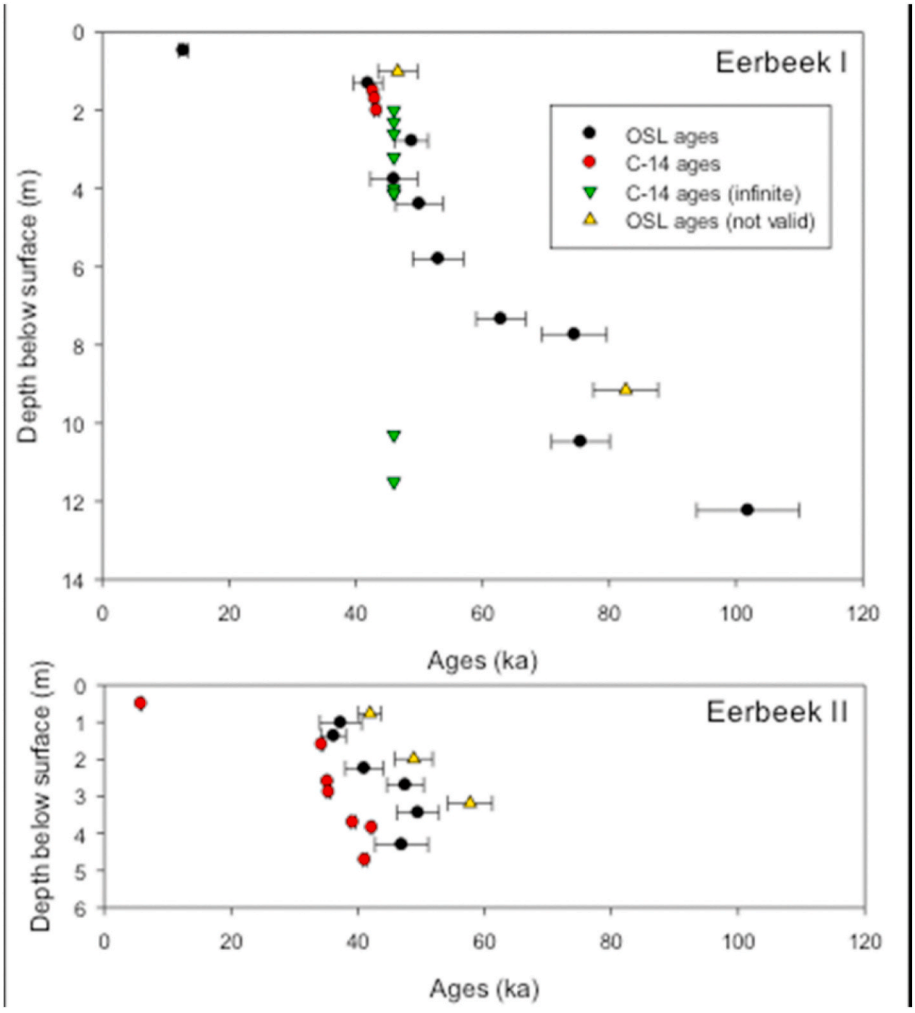


**Fig. 6.** $^{14}$C and OSL dating results measured for the Eerbeek-I and Eerbeek-II cores. Dates in ka calBP are before 1950 CE for $^{14}$C years and before 2009 CE for OSL years. Hence, the conventions for each of the methods are followed. The mutual age offset of 59 years is negligible.

**Table 8**
Fraction of plant remains (%mass) removed after each chemical pre-treatment and approximate$^{14}$C ages (in ka BP) of the removed material.

| Sample name | Depth (m) | Removed (%mass) after 2nd pre-treatment | $^{14}$C age (ka BP) removed fraction_2 | Removed (%mass) after 3rd pre-treatment | $^{14}$C age (ka BP) removed fraction_3 |
|---|---|---|---|---|---|
| Eerbeek I A | 1.51 | 22 | 10.5 | | |
| Eerbeek I C | 2.06 | 20 | 8.2 | | |
| Eerbeek I D | 2.36 | 21 | 30.4 | | |
| Eerbeek I H | 4.23 | 27 | 26.1 | | |
| Eerbeek II C | 2.63 | 20 | 22.3 | | |
| Eerbeek II D | 2.96 | 24 | 26.0 | | |
| Eerbeek II E | 3.79 | 25 | 29.0 | | |
| Eerbeek II F | 4.00 | 27 | 30.6 | 77 | 36.5 |

- For dating deposits older than 30 ka the OSL method is, in comparison with $^{14}$C dating, currently the most reliable dating method, as long as suitable sandy deposits are available.
- Additional dating methods are needed to verify obtained $^{14}$C datasets, especially for $^{14}$C dates older than 30 ka. If intercalations with sandy deposits are available from the same core, the OSL method is a reliable dating method to verify a$^{14}$C dataset.

## Declaration of competing interest

The authors declare that they have no known competing financial interests or personal relationships that could have appeared to influence the work reported in this paper.

## Acknowledgements

We like to thank the farmers at Eerbeek who allowed us to drill cores from their land, GeoDelft/Deltares for drilling the cores and Professor Tom Veldkamp, Land Dynamics Group, Wageningen University for funding of the drilling and core analysis. We thank Alice Veenendaal (NCL) for the OSL measurements and the laboratory-staff of CIO, University Groningen for the $^{14}$C measurements. A significant part of the OSL and $^{14}$C analyses in this study were funded by CAAS (Centre of Arts and Archaeological Sciences, Leiden University).

## Appendix A

**Table A.1**
Description of Eerbeek-I $^{14}$C samples.

| Sample name | Depth (m) | Core-slice weight (g) | Core material | Weight (g) of plant remains after 1st ABA | Description of dried material after ABA pretreatment |
|---|---|---|---|---|---|
| Eerbeek I A | 1.51 | 27 | Black/brown organic material | 0.51 | Small (~1 mm) brown plant remains. |
| Eerbeek I B | 1.75 | 25 | Black organic material | 0.63 | Small (~1 mm) brown plant remains and a few seeds (1–3 mm). |
| Eerbeek I C | 2.06 | 30 | Black organic material; pieces of wood | 0.44 | Small (~1 mm) brown plant remains. A 10 mm piece of tree material. |
| Eerbeek I D | 2.36 | 26 | Black/brown organic material; peat structure | 0.53 | Small (~2 mm) brown plant remains. |
| Eerbeek I E1 | 2.62 | 38 | Brown colour with sand and gravel | 0.38 | Small (~2 mm) brown plant remains and a few seeds (2 mm). |
| Eerbeek I E2 | 3.27 | 47 | Yellow sand with plant branches and roots | 0.06 | Small (~5 mm) brown plant remains. |
| Eerbeek I F | 3.47 | 8.5 | Yellow sand with plant branches and roots | <0.36 (no ABA) | |
| Eerbeek I G | 4.11 | 103 | Yellow sand and brown clay | 0.49 | Small (~2–10 mm) brown plant remains and a few seeds (1–3 mm); many of mica (~1 mm). |
| Eerbeek I H | 4.23 | | Sand and peat material | 0.37 | Small (~2–5 mm) brown plant remains and several seeds (1–3 mm); many of mica (~1 mm). |
| Eerbeek I I | 5.16 | 100 | Yellow sand with plant remains | <0.65 (no ABA) | |
| Eerbeek I J | 8.09 | | *No description* | <1 mg (no ABA) | |
| Eerbeek I K | 10.43 | | Black peat; tight structured | 0.94 | Small (~1–5 mm) brown and yellow plant remains and a few seeds (1 mm). |
| Eerbeek I M | 11.60 | | Black peat; tight structured | 0.82 | Small (~1–5 mm) brown and yellow plant remains and a few seeds (1–2 mm). |

**Table A.2**
Description of Eerbeek-II $^{14}$C samples.

| Sample name | Depth (m) | Core-slice weight (g) | Core material | Weight (g) of plant remains after 1st ABA | Description of dried material after ABA pretreatment |
|---|---|---|---|---|---|
| Eerbeek II A | 0.51 | | Sand, gravel | 0.02 | Light yellow-brown and a few black plant remains (<0.5 mm). |
| Eerbeek II B1 | 1.68 | | Red-brown sand; large size gravel. | 0.04 | Small (~1 mm) brown and yellow plant remains. |
| Eerbeek II B2 | 1.96 | 68 | Brown-grey sand; small size gravel. | <1 mg (no ABA) | |
| Eerbeek II C | 2.63 | 61 | Yellow sand, brown organic material; small size gravel. | 0.41 | Small (~2–5 mm) brown plant remains and a few seeds (1–3 mm). |
| Eerbeek II D | 2.96 | | Peat | 0.72 | Small (~1–3 mm) brown plant remains and a few seeds (1–3 mm). |
| Eerbeek II E | 3.79 | 48 | Peat with fine structure | 0.38 | Small (~2 mm) brown plant remains and many of mica (~1 mm). |
| Eerbeek II F | 4.00 | | Sand and peat | 0.46 | Small (~1–3 mm) brown plant remains and a few mica (~1 mm). |
| Eerbeek II G | 4.87 | 71 | Yellow sand with black (organic) particles. | 0.10 | Small (~1–3 mm) brown plant remains and many of mica (~1 mm). |

*Appendix B*

Pictures with examples of pre-treated plant remains, $^{14}C$ samples. Upper four: Eerbeek I-A and I–C, I-G and I–H. Lower four: Eerbeek II-A,and II-D, II-F and II-G. 'Eerbeek I-G' shows similar round-shaped seeds (3 mm diameter) as were measured for 'Eerbeek I–H'.

*Appendix C*

**Table C.1**
EA (%C), IRMS ($\delta^{13}C$; relative to VPDB and $\pm 1\sigma = 0.1‰$) and AMS ($F^{14}C$) measurement results of organic samples Eerbeek-II. '+' or '++' in the sample name indicates measurement of the material after additional chemical pre-treatments.

| Sample name | %C | $\delta^{13}C$ (‰) | Lab ID | $F^{14}C \pm 1\sigma$ (%) |
|---|---|---|---|---|
| Eerbeek-I | | | | |
| Eerbeek I A | 49.7 | −28.7 | GrA-52109 | 5.22 ± 0.07 |
| Eerbeek I A+ | 53.0 | −28.7 | GrA-57983 | 0.81 ± 0.04 |
| Eerbeek I B | 52.9 | −29.6 | GrA-52110 | 0.76 ± 0.04 |
| Eerbeek I C | 47.5 | −28.5 | GrA-52111 | 3.26 ± 0.06 |
| Eerbeek I C+ | 55.1 | −28.4 | GrA-57984 | 0.73 ± 0.04 |
| Eerbeek I C wood | 46.7 | −28.6 | GrA-52112 | 80.48 ± 0.34 |
| Eerbeek I D | 50.6 | −28.9 | GrA-52113 | 0.44 ± 0.03 |
| Eerbeek I D+ | 56.4 | −28.6 | GrA-57985 | 0.19 ± 0.03 |
| Eerbeek I E1 | 49.4 | −29.6 | GrA-52114 | 0.21 ± 0.03 |
| Eerbeek I E2 | 33.8 | −28.5 | GrA-52116 | 0.31 ± 0.03 |
| Eerbeek I G | 45.7 | −29.1 | GrA-52121 | 0.16 ± 0.03 |
| Eerbeek I H seed | 17.2 | −26.1 | GrA-49442 | 0.26 ± 0.06 |
| Eerbeek I H | 49.3 | −29.0 | GrA-48932 | 0.98 ± 0.03 |
| Eerbeek I H+ | 52.4 | −29.5 | GrA-57987 | 0.14 ± 0.03 |
| Eerbeek I K | 59.1 | −28.8 | GrA-48933 | 0.04 ± 0.04 |
| Eerbeek I M | 48.8 | −29.8 | GrA-49246 | 0.07 ± 0.02 |
| **Eerbeek-II** | | | | |
| Eerbeek II A | 53.5 | −30.0 | GrA-48936 | 53.02 ± 0.24 |
| Eerbeek II B1 | – | −28.2 | GrA-52570 | 2.68 ± 0.05 |
| Eerbeek II B1+ | 53.0 | −28.0 | GrA-57990 | 2.29 ± 0.05 |
| Eerbeek II C | 51.5 | −28.4 | GrA-52120 | 2.60 ± 0.05 |
| Eerbeek II C+ | 54.5 | −27.0 | GrA-57992 | 2.02 ± 0.05 |
| Eerbeek II D | 50.5 | −29.4 | GrA-48937 | 2.45 ± 0.04 |
| Eerbeek II D+ | 50.8 | −29.3 | GrA-57993 | 1.99 ± 0.05 |
| Eerbeek II E | 51.0 | −29.3 | GrA-52119 | 1.68 ± 0.04 |
| Eerbeek II E+ | 51.0 | −31.3 | GrA-57994 | 1.34 ± 0.04 |
| Eerbeek II F | 51.1 | −28.9 | GrA-48938 | 1.32 ± 0.03 |
| Eerbeek II F+ | 52.9 | −29.0 | GrA-57995 | 1.03 ± 0.04 |
| Eerbeek II F++ | 54.0 | −28.5 | GrA-58445 | 0.90 ± 0.03 |
| Eerbeek II G | – | −29.4 | GrA-52572 | 1.30 ± 0.04 |
| Eerbeek II G+ | 50.3 | −29.3 | GrA-57996 | 1.07 ± 0.04 |

## References


Aalbersberg, G., Litt, T., 1998. Multiproxy climate reconstructions for the eemian and early weichselian. J. Quat. Sci. 13 (5), 367–390.

Aerts-Bijma, A.T., van der Plicht, J., Meijer, H.A.J., 2001. Automatic AMS sample combustion and $CO_2$ collection. Radiocarbon 43 (2A), 293–298.

Aitken, M.J., 1985. Thermoluminescence Dating. Academic Press, Orlando, FL.

Anechitei-Deacu, V., Timar-Gabor, A., Thomsen, K.J., Buylaert, J.-P., Jain, M., Bailey, M., Murray, A.S., 2018. Single and multi-grain OSL investigations in the high dose range using coarse quartz. Radiat. Meas. 120, 124–130.

Bailey, R.M., Arnold, L.J., 2006. Statistical modelling of single grain quartz De distributions and an assessment of procedures for estimating burial dose. Quat. Sci. Rev. 25, 2475–2502.

Bakker, M.A.J., Van der Meer, J.J.M., 2003. Structure of a Pleistocene push moraine revealed by GPR: the eastern Veluwe Ridge, The Netherlands. In: Bristow, C.S., Joi, H.M. (Eds.), Ground Penetrating Radar in Sediments, vol. 211. Geological Society, London Special Publications, pp. 143–151.

Bateman, M.D., van Huissteden, J., 1999. The timing of last glacial periglacial and aeolian events, Twente, Eastern Netherlands. J. Quat. Sci. 14, 277–283.

Ballarini, M., Wintle, A.G., Wallinga, J., 2006. Spatial variation of dose rate from beta sources as measured using single grains. Ancient TL 24, 1–7.

Begemann, H.K.S.P., 1974. Bull. Int. Assoc. Eng. Geol. 10, 35. https://doi.org/10.1007/BF02634629.

Briant, R.M., Bateman, M.D., Russell Coope, G., Gibbard, P.L., 2005. Climatic control on quaternary fluvial sedimentology of a fenland basin river, england. Sedimentology 52, 1397–1423.

Briant, R.M., Bateman, M.D., 2009. Luminescence dating indicates radiocarbon age underestimation in late Pleistocene fluvial deposits from eastern England. J. Quat. Sci. 24 (8), 916–927.

Briant, R.M., Brock, F., Demarchi, B., Langford, H.E., Penkman, K.E.H., et al., 2018. Improving chronological control for environmental sequences from the last glacial period. Quat. Geochronol. 43, 40–49.

Bronk Ramsey, C., 2009. Bayesian analysis of radiocarbon dates. Radiocarbon 51 (1), 337–360.

Botter-Jensen, L., Andersen, C.E., Duller, G.A.T., Murray, A.S., 2003. Developments in radiation, stimulation and observation facilities in luminescence measurements. Radiat. Meas. 37, 535–541.

Busschers, F.S., van Balen, R.T., Cohen, K.M., Kasse, C., Weerts, H.J.T., Wallinga, J., Bunnik, F.P.M., 2008. Response of the Rhine-Meuse fluvial system to Saalian ice-sheet dynamics. Boreas 37 (3), 377–398.

Buylaert, J.P., Jain, M., Murray, A.S., Thomsen, K.J., Thiel, C., Sohbati, R., 2012. A robust feldspar luminescence dating method for Middle and Late Pleistocene sediments. Boreas 41, 435–451.

Buylaert, J.P., Murray, A.S., Gebhardt, A.C., Sohbati, R., Ohlendorf, C., Thiel, C., et al., 2013. Luminescence dating of the PASADO coree 5022-1D from Laguna Potrok Aike (Argentina) using IRSL signals from feldspar. Quat. Sci. Rev. 71, 70–80.

Chamberlain, E., Wallinga, J., 2019. Fluvial sediment pathways enlightened by OSL bleaching of river sediments and deltaic deposits. Earth Surface Dynamics. https://doi.org/10.5194/esurf-2018-76.

Chamberlain, E., Wallinga, J., Shen, Z., 2018b. Luminescence age modeling of variably-bleached sediment: model selection and input. Radiat. Meas. https://doi.org/10.1016/j.radmeas.2018.06.007.

Chamberlain, E.L., Tornqvist, T.E., Shen, Z.X., Mauz, B., Wallinga, J., 2018a. Anatomy of Mississippi Delta growth and its implications for coastal restoration. Science Advances 4. https://doi.org/10.1126/sciadv.aar4740.

Cunningham, A.C., Wallinga, J., 2010. Selection of integration time intervals for quartz OSL decay curves. Quat. Geochronol. 5, 657–666. https://doi.org/10.1016/j.quageo.2010.08.004.

Cunningham, A.C., Wallinga, J., 2012. Realizing the potential of fluvial archives using robust OSL chronologies. Quat. Geochronol. 12, 98–106. https://doi.org/10.1016/j.quageo.2012.05.007.

Crombé, P., Van Strydonck, M., Boudin, M., Van den Brande, T., Derese, C., Vandenberghe, D.A.G., et al., 2012. Absolute dating ($^{14}C$ and OSL) of the formation of coversand ridges occupied by prehistoric hunter-gatherers in new Belgium. Radiocarbon 54 (3–4), 715–726.

Derese, C., Vandenberghe, D., Paulissen, E., Van den haute, 2009. Revisiting a type locality for Late Glacial aeolian sand deposition in NW Europe: optical dating of the dune complex at Opgrimbie (NE Belgium). Geomorphology 109, 27–35.

De Mulder, E.F.J., Geluk, M.C., Ritsema, I.L., Westerhoff, W.E., Wong, T.E., 2003. De Ondergrond Van Nederland 379. Wolters-Noordhoff bv Groningen/Houten, the Netherlands, ISBN 9001605141.

Demuro, M., Roberts, R.G., Froese, D.G., Arnold, L.J., Brock, F., Bronk Ramsay, C., 2008. Optically stimulated luminescence dating of single and multiple grains of quartz from perennially frozen loess in western Yukon Territory, Canada: comparison with radiocarbon chronologies for the late Pleistocene Dawson tephra. Quat. Geochronol. 3, 346–364.

Den Otter, C., 1989. Rapport m.b.t. Groeve Coldenhove, Eerbeek (Ontsluitingen archief). Rijksgeologische Dienst Haarlem.

De Vries, H., 1958. Radiocarbon dates for upper Eem and Würm-interstadial samples. Quaternary Science Journal 9 (1), 1–8.

DINO, 2014. https://www.dinoloket.nl/en/subsurface-data. (Accessed 24 September 2020).
Douglas, B.J., Olsen, R.S., 1981. Soil classification using electric cone penetrometer. In: Proceedings of Conference on Cone Penetration Testing and Experience, vol. 26. St. Louis 30 October 1981, 209-227.
Duller, G.A.T., 2003. Distinguishing quartz and feldspar in single grain luminescence measurements. Radiat. Meas. 37, 161–165.
Duller, G.A.T., 2008. Single-grain optical dating of Quaternary sediments: why aliquot size matters in luminescence dating. Boreas 37, 589–612.
Galbraith, R.F., Roberts, R.G., Laslett, G.M., Yoshida, H., Olley, J.M., 1999. Optical dating of single and multiple grains of quartz from Jinmium rock shelter, northern Australia: Part 1, Experimental design and statistical models. Archaeometry 41, 339–364. https://doi.org/10.1111/j.1475-4754.1999.tb00987.x.
Guérin, G., Mercier, N., Adamiec, G., 2011. Dose-rate conversion factors: update. Ancient TL 29, 5–8.
Guérin, G., Christophe, C., Philippe, A., Murray, A.S., Thomsen, K.J., Tribolo, C., Urbanova, P., Jain, M., Guibert, P., Mercier, N., Kreutzer, S., Lahaye, C., 2017. Absorbed dose, equivalent dose, measured dose rates, and implications for OSL age estimates: introducing the Average Dose Model. Quat. Geochronol. 41, 163–173.
Huntley, D.J., Godfrey-Smith, D.I., Thewalt, M.L.W., 1985. Optical dating of sediments. Nature 313, 105–107.
Kasse, C., 2002. Sandy aeolian deposits and environments and their relation to climate during the Last Glacial Maximum and Lateglacial in northwest and central Europe. Prog. Phys. Geogr. 26 (4), 507–532.
Kasse, C., Bohncke, S.J.P., Vandenberghe, J., 1995. Fluvial perioglacial environments, climate and vegetation during the Middle Weichselian in the Northern Netherlands with special reference to the Hengelo interstadial. Meded. Rijks Geol. Dienst, Nieuwe Ser. (Neth) 52, 387–414.
Kliem, P., Enters, D., Hahn, A., Ohlendorf, C., Lisé-Pronovost, A., St-Onge, G., et al., 2013. Lithology, radiocarbon chronology and sedimentological interpretation of the lacustrine record from Laguna Potrok Aike, southern Patagonia. Quat. Sci. Rev. 71, 54–69.
Kolstrup, E., Wijmstra, T.A., 1977. A palynological investigation of the Moershoofd, Hengelo and Denekamp interstadials in The Netherlands. Geol. Mijnbouw 56, 85–102.
Kolstrup, E., Murray, A., Possnert, G., 2007. Luminescence and radiocarbon ages from laminated Lateglacial Aeolian sediments in western Jutland, Denmark. Boreas 36, 315–325.
Libby, W.F., 1952. Radiocarbon Dating. University Press, Chicago. Re-issued 1965.
Lunne, T., Robertson, P.K., Powell, J.J.M., 1997. Cone Penetration Testing in Geotechnical Practice, first ed. E & FNSpon Press, Abingdon.
Maarleveld, G.C., 1949. Over erosiedalen van de Veluwe, 2e reeks LXVI. KNAG Tijdschrift, pp. 133–143.
Madsen, A.T., Murray, A., Andersen, T., Pejrup, M., Breuning-Madsen, H., 2005. Optically stimulated luminescence dating of young estuarine sediments: a comparison with $^{210}$Pb and $^{137}$Cs dating. Mar. Geol. 214, 251–268. https://doi.org/10.1016/j.margeo.2004.10.034.
Madsen, A.T., Murray, A.S., 2009. Optically stimulated luminescence dating of young sediments: a review. Geomorphology 109 (1), 3–16.
Magee, J.W., Bowler, J.M., Miller, G.H., Williams, D.L.G., 1995. Stratigraphy, sedimentology, chronology and palaeo-hydrology of the quaternary lacustrine deposits at madigan gulf, lake eyre, south Australia. Palaeogeogr. Palaeoclimatol. Palaeoecol. 113, 3–42.
Mejdahl, V., 1979. Thermoluminescence dating: beta-dose attenuation in quartz grains. Archaeometry 21, 61–72. https://doi.org/10.1111/j.1475-4754.1979.tb00241.x.
Mook, W., Streurman, H.J., 1983. Physical and chemical aspects of radiocarbon dating. In: Mook, W.G., Waterbolk, H.T., Pact8 (Eds.), Preceedings of the International Groningen Symposium $^{14}$C and Archaeology, pp. 31–55.
Mook, W.G., van der Plicht, J., 1999. Reporting $^{14}$C activities and concentrations. Radiocarbon 41 (3), 227–239.
Murray, A.S., Wintle, A.G., 2000. Luminescence dating of quartz using an improved single-aliquot regenerative-dose protocol. Radiat. Meas. 32, 57–73.
Murray, A.S., Wintle, A.G., 2003. The single aliquot regenerative dose protocol: potential for improvements in reliability. Radiat. Meas. 37, 377–381. https://doi.org/10.1016/S1350-4487(03)00053-2.
Olsson, I.U., 1989. The $^{14}$C Method—Its Possibilities and Some Pitfalls, vol. 24. PACT Publications, pp. 161–177.
Prescott, J.R., Hutton, J.T., 1994. Cosmic ray contributions to dose rates for luminescence and ESR dating: large depths and long-term time variations. Radiat. Meas. 23, 497–500. https://doi.org/10.1016/1350-4487(94)90086-8.
Preusser, F., Degering, D., Fuchs, M., Hilgers, A., Kadereit, A., Klasen, N., Krbetschek, M., Richter, D., Spencer, J.Q.G., 2008. Luminescence dating: basics, methods and applications. Eiszeitalter und Gegenwart. Quaternary Science Journal 57, 95–149.
Reimann, T., Notenboom, P.D., De Schipper, M.A., Wallinga, J., 2016. Testing for sufficient signal resetting during sediment transport using a polymineral multiple-signal luminescence approach. Quat. Geochronol. 25, 26–36. https://doi.org/10.1016/j.quageo.2014.09.002.
Reimer, P.J., Bard, E., Bayliss, A., et al., 2013. IntCal13 and Marine13 Radiocarbon age calibration curves 0-50.000 years cal BP. Radiocarbon 55 (4), 1869–1887.
Rhodes, E., Ramsey, C.B., Outram, Z., Batt, C., Willis, L., Dockrill, S., Bond, J., 2003. Bayesian methods applied to the interpretation of multiple OSL dates: high precision sediment ages from Old Scatness Broch excavations, Shetland Isles. Quat. Sci. Rev. 22, 1231–1244. https://doi.org/10.1016/S0277-3791(03)00046-5.
Ruegg, G.H.J., 1979. Sedimentstructureel en granulometrisch onderzoek van afzettingen ontsloten in een bouwput bij Drachten. Rijks Geologische Dienst, Haarlem. Sedimentologische Afdeling, Rapport 43.
Stevenson, F.J., 1994. Humus Chemistry. Genesis, Composition, Reactions, second ed. Wiley & Sons, New York.
Stuiver, M., Polach, H.A., 1977. Discussion: reporting of $^{14}$C data. Radiocarbon 19 (3), 355–363.
Thomsen, K.J., Murray, A.S., Botter Jensen, L., 2005. Sources of variability in OSL dose measurements using single grains of quartz. Radiat. Meas. 39, 47–61.
Újvári, G., Molnár, M., Novothny, Á., Páll-Gergely, B., Kovács, J., Várhegyi, 2014. AMS $^{14}$C and OSL/IRSL dating of the Dunaszekcsó loess sequence (Hungary): chronology for 20 – 150 ka and implications for establishing reliable age – depth models for the last 40 ka. Quat. Sci. Rev. 106, 140–154.
Van den Berg, M.W., Beets, D., 1987. Saalian glacial deposits and morphology in The Netherlands. In: Van der Meer, J.J.M. (Ed.), Tills and Glaciotectonics. Balkema, Rotterdam, pp. 235–251.
van der Meer, J.J.M., Slotboom, R.T., De Vires-Bruynsteen, I.M.E., 1984. Lithology and palynology of Weichselian alluvial fan deposits near Eerbeek, The Netherlands. Boreas 13, 393–402.
van der Plicht, J., Hogg, A., 2006. A note on reporting radiocarbon. Quat. Geochronol. 1, 237–240.
van der Plicht, J., Wijma, S., Aerts, A.T., Pertuisot, M.H., Meijer, H.A.J., 2000. Status report: the Groningen AMS facility. Nucl. Instrum. Methods Phys. Res. 172 (B), 58–65.
Vandenberghe, D., De Corte, F., Buylaert, J.P., Kucera, J., Van den haute, P., 2008. On the internal radioactivity of quartz. Radiat. Meas. 43, 771–775.
Vandenberghe, D., Kasse, C., Hossain, S.M., De Corte, F., Van den haute, P., Fuchs, M., Murray, A.S., 2004. Exploring the method of optical dating and comparison of optical and 14C ages of Late Weichselian coversands in the southern Netherlands. J. Quat. Sci. 19 (1), 73–86.
Viveen, W., 2005. The Internal Build-Up of the Alluvial Fan Near Eerbeek within a Climatic Context. BSc thesis Wageningen University, Wageningen, The Netherlands, p. 101.
Viveen, W., Zevallos-Valdivia, L., Sanjurjo-Sanchez, J., 2019. The influence of centennial-scale variations in the South Americal Summer Monsoon and base level fall on Holocene fluvial systems in the Peruvian Andes. Global Planet. Change 176, 1–22.
Wallinga, J., Bos, I.J., 2010. Optical dating of fluvio-deltaic clastic lake-fill sediments. A feasibility study in the Holocene Rhine delta (western Netherlands). Quat. Geochronol. 5, 602–610. https://doi.org/10.1016/j.quageo.2009.11.001.
Wallinga, J., van Mourik, J.M., Schilder, M.L.M., 2013. Identifying and dating buried micropodzols in Subatlantic polycyclic drift sands. Quat. Int. 306, 60–70.
Wallinga, J., Murray, A.S., Bøtter-Jensen, L., 2002. Measurement of the dose in quartz in the presence of feldspar contamination. Radiat. Protect. Dosim. 101, 367–370.
Weerts, H.J.T., 1996. Complex confining layers. Architecture and hydraulic properties of Holocene and LateWeichselian deposits in the fluvial Rhine Meuse delta, The Netherlands. Nederl. Geogr. Stud. 213, 1–189.
Wintle, A.G., Adamiec, G., 2017. Optically stimulated luminescence signals from quartz: a review. Radiat. Meas. 98, 10–33.
Wintle, A.G., 2008. Luminescence dating: where it has been and where it is going. Boreas 37, 471–482.
Zaccone, C., Sanei, H., Outridge, P.M., Miano, T.M., 2011. Studying the humification degree and evolution of peat down a Holocene bog profile (Inuvik, NW Canada): a petrological and chemical perspective. Org. Geochem. 42, 399–408.